WARSHIP CLASSIFICATION FROM DISTANT VIEW USING DYNAMIC TIME WARPING AND K-NN

SUB.LT. BUNCHA CHUAYSI

A THESIS SUBMITTED IN PARTIAL FULFILLMENT
OF THE REQUIREMENTS FOR
THE DEGREE OF MASTER OF SCIENCE
(TECHNOLOGY OF INFORMATION SYSTEM MANAGEMENT)
FACULTY OF GRADUATE STUDIES
MAHIDOL UNIVERSITY
2013

Thesis
entitled
WARSHIP CLASSIFICATION FROM DISTANT VIEW
USING DYNAMIC TIME WARPING AND K-NN

….………………………………………..
Sub.Lt. Buncha Chuaysi
Candidate

………………………….………………
Lect. Supaporn Kiattisin,
Ph.D. (Electrical and Computer
Engineering)
Major advisor

………………………….………………
Asst. Prof. Adisorn Leelasantitham,
Ph.D. (Electrical Engineering)
Co-advisor

………………………….………………
Lect. Waranyu Wongseree,
Ph.D. (Electrical Engineering)
Co-advisor

………………………….………
Prof. Banchong Mahaisavariya,
M.D., Dip. (Thai Board of Orthopedics)
Dean
Faculty of Graduate Studies,
KMUTT University

………………………….………………
Lect. Supaporn Kiattisin,
Ph.D.
(Electrical and Computer Engineering)
Program Director
Master of Science Program in
Technology of Information System
Management
Faculty of Engineering,
Mahidol University

Thesis
entitled
WARSHIP CLASSIFICATION FROM DISTANT VIEW
USING DYNAMIC TIME WARPING AND K-NN

was submitted to the Faculty of Graduate Studies, Mahidol University
for the degree of Master of Science
(Technology of Information System Management)
on
April 10, 2013

………………….…..…………………
Sub.Lt. Buncha Chuaysi
Candidate

………………….…..…………………
Asst.Prof.Bunlur Emaruechi,
Ph.D.
(Environment Systems Engineering)
Chair

………………….…..…………….. ………….…..………………...…
Lect. Supaporn Kiattisin, Asst. Prof. Adisorn Leelasantitham,
Ph.D. (Electrical and Computer Ph.D. (Electrical Engineering)
Engineering) Member
Member

………………………....……… ………………….…..…………………
Lect.Waranyu Wongseree, Asst.Prof.Werapon Chiracharit,
Ph.D. (Electrical Engineering) Ph.D. (Electrical and Computer
Member Engineering)
  Member

……………………...…………. ………………………..……………
Prof. Banchong Mahaisavariya, Lect. Worawit Israngkul,
M.D., Dip (Thai Board of Orthopedics) M.S. (Technical Management)
Dean Dean
Faculty of Graduate Studies Faculty of Engineering
Mahidol University Mahidol University

ACKNOWLEDGEMENTS

Sub.Lt. Buncha Chuaysi

WARSHIP CLASSIFICATION FROM DISTANT VIEW USING DYNAMIC TIME WARPING AND K-NN

SUB.LT. BUNCHA CHUAYSI   5436450 EGTI / M

M.Sc. (TECHNOLOGY OF INFORMATION SYSTEM MANAGEMENT)

THESIS ADVISORY COMMITTEE: SUPAPORN KIATTISIN, Ph.D., ADISORN LEELASANTITHAM, Ph.D., WARANYU WONGSEREE, Ph.D.

ABSTRACT

This study proposes a method to classify warships from distant view images which has high importance for military information systems and military operations. In this work, we present different tangent-angles (DOT) along the boundary of distant view images as a descriptive feature. This method is invariant under transition, scaling and rotation.

To prove this, we applied the method to warship classification by using a side view of distant view images for data input. We reduced the dimensions of data by using a piecewise aggregate approximation (PAA) algorithm to speed up the computation. Finally, we compared the dynamic time warping (DTW) to Euclidean distance (ED) and k-nearest neighbor (k-NN) were used for measuring similarity and classification.

To evaluate the performance of the proposed method, a confusion matrix and receiver operating characteristic (ROC) curve were used. In conclusion, this approach provided a good classification rate for DTW.

KEY WORDS: SHAPE FEATURE EXTRACTION / DIFERANCE OF TANGENT / PIECEWISE AGGREGATE APPROXIMATION / DYNAMIC TIME WARPING / K-NEAREST NEIGHBOR

74 pages

การจำแนกประเภทเรือรบจากภาพระยะไกลด้วยเทคนิค DYNAMIC TIME WARPING และ k-NN

WARSHIP CLASSIFICATION FROM DISTANT VIEW USING DYNAMIC TIME WARPING AND K-NN

ร.ต.บัญชา ช่วยสี 5436450 EGTI/M

วท.ม. (เทคโนโลยีการจัดการระบบสารสนเทศ)

คณะกรรมการที่ปรึกษาวิทยานิพนธ์: สุภาภรณ์ เกียรติสิน, Ph.D., อดิศร ลีลาสันติธรรม, Ph.D.,
วรัญญู วงษ์เสรี, Ph.D.

บทคัดย่อ

งานวิจัยนี้มีวัตถุประสงค์เพื่อสร้างแนวคิดในการจำแนกประเภทเรือรบจากภาพ
ระยะไกล (distant view) ซึ่งภาพลักษณะดังกล่าวมีความสำคัญต่อการพัฒนาระบบสารสนเทศเพื่อ
การตัดสินใจในทางทหาร ซึ่งการวิจัยนี้ได้นำเสนอการสกัดคุณสมบัติของภาพด้วยการคำนวณหา
ผลต่างของมุมแทน (difference of tangent-angles: DOT) ตามแนวเส้นขอบของเรือ โดยเทคนิค
ดังกล่าวนี้คงทนต่อการเปลี่ยนแปลงของตำแหน่งวัตถุในภาพ การลด เพิ่มขนาด และ การหมุน ของ
วัตถุ นอกจากนี้ได้ลดจำนวนข้อมูลด้วยเทคนิค PAA เพื่อเพิ่มความเร็วในการประมวลผล การศึกษา
นี้ได้เปรียบเทียบการวัดความแตกต่างระหว่างการใช้เทคนิคไดนามิคไทม์วอร์ปปิ้ง และ เทคนิค
ยูคลิด โดยในขั้นการจำแนกประเภทเรือรบ ใช้เทคนิคเนียเรสเนเบอร์ ซึ่งเป็นที่นิยมสำหรับการ
จำแนกข้อมูลที่มีลักษณะเหมือนข้อมูลอนุกรมเวลา (Time series)

ผลของการศึกษาถูกวิเคราะห์ด้วย confusion matrix และ ROC พบว่าเทคนิคไดนามิค
ไทม์วอร์ปปิ้ง ให้ผลในการจำแนกประเภทเรือรบจากภาพระยะไกลที่ดี

74 หน้า

CONTENTS

CONTENTS (cont.)

LIST OF TABLES

LIST OF FIGURES

LIST OF FIGURES (cont.)

CHAPTER I
INTRODUCTION

1.1 Background and Problems

Classification of an object as a warship from a distant view is one type of important information for Network-Centric Warfare (NCW). It has high level of importance for military operations decisions. Military personnel need effective and accurate information for management procedures to ensure that correct information is available for deciders to make informed decisions [1].

To classify warship, many approaches have been advocated e.g. Synthetic Aperture Radar (SAR), Inverse Synthetic Aperture Radar (ISAR) and some based on Forward Looking Infra-Red (FLIR), sonar images and magnetic signatures. To obtain SAR, ISAR, FLIR, and sonar data images, we need large equipment that does not fit in small vehicles or aircraft. Therefore, these are not practical for field operations usage.

Normally, warship should be identified while they are at a distance presenting only a silhouette to the observer. Fortunately, with new technology, we have the capability to insert small cameras into small vehicles, aircraft, and robots to take pictures and transmit the images for processing.

This study presents an algorithm using distant view images taken by camera as input data to classify warships by the Difference of Tangent-angles (DOT) on the superstructure boundary for the purpose of identifying their descriptive features. In addition, the invariant under translation, scaling, and rotation were also studied.

1.2 Objectives

The objective of this work is

1.2.1 To develop feature extraction method from distance view images.

1.2.2 To study the theory of Dynamic Time Warping, k-nearest neighbor and Piecewise Aggregate Approximation.

1.2.3 To speed up the feature matching process.

1.3 Scope of Work

The scope of this work included the following:

1.3.1 Sample demonstrated in this research were prototypes.

1.3.2 Silhouette images file format PNG, JPG or BMP.

1.3.3 This research involves image preprocessing.

1.4 Expected Result

The outcomes of this work proved that the feature extraction method would be good for warship classification and is invariant under translation, scaling, and rotation. The advantage and disadvantage points of this method would be mentioned.

CHAPTER II
LITERATURE REVIEW

2.1 Overview

Classification of the warship, references [2], [3], [4], and [5], discuss the ship recognition by Synthetic Aperture Radar (SAR) and Inverse Synthetic Aperture Radar (ISAR) and references [6], [7], and [8] discuss the recognition by Forward Looking Infra-Red (FLIR) images. Reference [9] discusses the use of sonar images and reference [10] discusses the use of magnetic signatures for data input. To obtain ISAR, FLIR, and sonar data images, we need large equipment that does not fit in small vehicles or aircraft and is therefore not practical for field operations usage. Fortunately, with new technology, we have the capability to insert small cameras into small vehicles, aircraft, and robots to take pictures and transmit the images for processing.

Normally, warship should be identified while they are at a distant where they would present only a silhouette to the observer. The type/classes of warships should be determined from their silhouette long before their hull numbers or names.

This study presents an algorithm using distant view images taken by camera as data input to classify warships by the Different of Tangent-angles (DOT) on the superstructure boundary for the purpose of identifying their descriptive features. To classify classes of warships with similar superstructures, we applied the dynamic time warping (DTW) for similar measurements, decreasing the computation time and reducing size of the data set by the use of the Piecewise Aggregate Approximation (PAA) algorithm. The last process for effective classification, the k-nearest neighbor (k-NN) algorithm for classification was used. This algorithm proves the classification accuracy rate to be invariant under translation, scaling, and rotation of images.

This chapter has been organized from many literature reviews follows: First, review on warship characteristic and related work for warship recognition. Next is summary of feature extractions that focused on silhouette and shape. From feature

extractions and our select method, we studied on time series. And the last is detail of main algorithm: PAA, DTW and k-NN.

2.2 Warship

All warships are designed and built to perform a common duty constitute a type of warship. Within each type of warship, there are classes or groups of ships built with a similar design. Specialized charts, reference books, and qualified specialists would be used as references for the different classes [2].

The most important feature for recognition is the visual impact of hulls, masts, radar aerials, funnels, and major weapons systems. There are nine major types of warships [11], namely:

Submarines

Aircraft Carriers

Cruisers

Destroyers

Frigates

Corvettes

Patrol Forces

Amphibious Forces

Mine Warfare Forces

The description in each type and example hulls would be show.

Table 2.1 describes the example hulls of each warship type and main features description.

Table 2.1 Major types of warship and recognized features

Warship Type	Characteristic and Recognized Features
Aircraft Carriers	Aircraft Carriers are generally the largest warships, flight deck give a distinct appearance. The superstructure island is the prominent feature, the other features are : - Squared 'chunky' island aft of mid ships - Air search radar - atop bridge - Starboard side, crane - Mid island - Twin funnel, one aft of bridge, - one aft of mainmast - CIWS mountings, - SAM launchers mounted port and starboard
Cruisers	Cruisers are multi-mission anti-air, anti-submarine, anti-surface and capable of supporting carriers. The trend in modern cruisers features tall, solid towers amidships and cylindrical stacks. The bow section contains weapons and electronics equipment. - Measurement about 550 – 700 feet in length - Displace from 7,000 – 15,000 tons

Table 2.1 Major types of warship and recognized features (cont.)

Warship Type	Characteristic and Recognized Features
Destroyers	Destroyers are versatile, multipurpose with - high bow with sweeping forecastle aft of bridge - twin, black-capped funnels angled astern - missile launchers, triple torpedo, mortar launcher - lamp fire control - air/surface search radar - tall superstructure - larger flight deck - helicopter hangar aft of mid ships - Measurement about 400 – 600 feet in length - Displace from 3,000 – 8,000 tons
Frigates	Frigates fall into the general category of smaller major combatants. - long slim hull with a high bow, - low in water - tall flat bridge structure - large, low funnel aft of mid ships - forward superstructure with enclosed mainmast at after end - flight deck with quarterdeck below - mid ships superstructure with pyramid mainmast at after end - Measurement about 300 – 400 feet in length - Displace from 1,500 – 4,000 tons

Table 2.1 Major types of warship and recognized features (cont.)

Warship Type	Characteristic and Recognized Features
Corvettes	- flat roofs - continuous main deck from stem to stem - high bow - low freeboard - short forecastle - no helicopter platform - gun mounting in A position -pyramid mainmast atop center of main superstructure
Patrol Forces	- small bridge forward of mid ships - high bow, low sloping forecastle - low freeboard - gun mounting in A, X and Y position - fire control radar - tall lattice at after end of bridge superstructure - high superstructure - steeped down at after end
Mine Warfare Forces	- 20mm/70 gun mounting - high bow, stepped, smooth contoured superstructure - low freeboard with continuous main deck from stem to stem - small square structure on afterdeck - square sectioned funnel with sloping top sited mid ships - small crane on quarterdeck - low superstructure from forecastle aft of quarterdeck

Table 2.1 Major types of warship and recognized features (cont.)

Warship Type	Characteristic and Recognized Features
Amphibious	Amphibious are designed to move combat personnel and equipment ashore. The boxlike superstructure can be identified. - Measurement about 800 – 8500 feet in length - Displace from 28,000 – 40,000 tons

The differences between the shapes of various ships mainly lie in their superstructures, while the differences of the ship bodies are slight. Fig. 1 shows coding of features in a distant view of a warship. The features are coded as follows [11]:

G: Gun	Gs: Gun (small)	C: Crane
D: Director	DR: Director (Raised)	B: Bubble
M: Mast	F: Funnel	L: Launcher
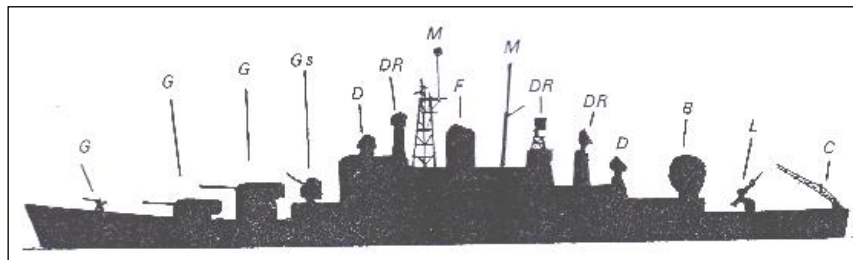
Figure 2.1 Example of coded features on a distant view of a warship [11]

There are many classes within each type of warship, each with similar superstructure as shown in Figure 2.2
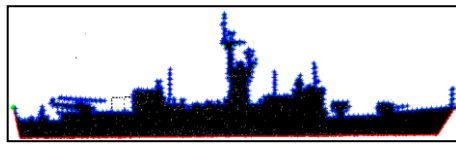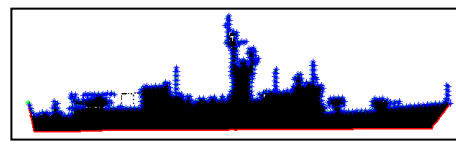
DAMYAT   PHUTTHAYOTFA

Figure 2.2 Warship Type: Frigates, Class: Knox

We found many related works on warship classification during the literature reviews. Early work on ship and warship classification, reference [12] uses coordinates of contour turn points from the silhouette's boundary. This method is noise sensitive and variant under translation, scaling, and rotation.

Based on SAR and ISAR, reference [2] discusses Principal Components Analysis (PCA) based on SAR images that produces fair results, but results are required to be tested with a larger data set. References [3], [4] work with ISAR and [5] works with SAR images. Reference [4] and [5] are based on 3D models, instead of real data. Reference [6] classifies satellite synthetic aperture radar (SAR) images of ships by moment invariants with two stage classification, presented to reduce the computation. By using the moment invariants as descriptive feature of ship's silhouettes and the 1-NN classifier based on SAR images. The results of the calculation of superstructure moment invariants as a descriptor have better discriminability and accuracy than general moment invariants, which are calculated for the entire the ship.

Reference [13] uses real data from radar ship images for target recognition. Fourier-modified discrete Mellin transform (F-MDMT) is used to transform the images and they are compared with two classifiers,; the first is back-propagation neural networks that require long training times, and the second is Learning Vector Quantization (LVQ), which is considered more favorable with classification accuracy up to 93% for ship type.

Based on FLIR image, reference [7] reports on two experimental systems for ship classification; the edge histogram approach and the neural network approach. They used moment invariants as input to training in the neural network with an

accuracy of 85.4% in determining ship type. However, the FLIR images are required to eliminate common artifacts such as ship shadows, reflections on the sea surface and heat from stacks. Reference [8] presents a method of ship classification based on covariance of discrete wavelets of ships images using a probabilistic neural network, which achieves an 87.5% correct classification rate.

Reference [9] presents the low-cost system work on passive sonar signals and Self-Organising Maps (SOM), the system take a very long time to training process.

Based on image, reference [14] present ship recognition techniques using color remote sensing imagery, obtaining a good classification rate. Reference [15] uses optical images as input data for Scale Invariant Feature Transform (SIFT) algorithm, which measures the distance between vectors. This method is invariant to scaling, rotation, and availability of only a partial view. The result provides excellent recognition rates, but data images must be sufficiently detailed for the SIFT and computation is very expensive. Reference [16] works with side views of image silhouettes using Curvature Scale Space (CSS) representation and compares these by Recursive Matching Matrix (RMM). Accuracy close to 80 % is obtained with a viewpoint angle near 90 degrees and variations within ± 10 degrees. Rotations larger than 10 degrees would result in misidentification. Reference [17] study offline ship recognition using model based of ships silhouette images. By using moment invariants and minimum distance feature vector, the sensitivity of moment invariants is affected by noise.

Summary of reference [2-17] based on data input, feature and invariant under translation, scaling and rotation (TSR) as shown in the table 2.2.

Table 2.2 Summary of warship classifications

Data (image)	Feature	Learning method	Output	Invariant
RADAR [13]	F-MDMT	ANN, LVQ	Types	N/A
SAR [2]	PCA	Euclidean	Classes	N/A
[5]	3D models	Compared	-	N/A
[6]	moment	1-NN	Types	TSR
ISAR [3]	Multi-feature	Compared	Classes	N/A
[4]	Range-doppler, 3D	Compared	Classes	N/A
FLIR [7]	Edge, Moment, 3D	Compared, ANN	Classes	TSR
Sonar [9]	SOM	ANN	-	N/A
Magnetic[10]	Magnetic	ANN	Classes	N/A
Remote sensing [14]	moment	k-NN	-	TSR
Optical [15]	SIFT	Feature matching	Classes	TSR, partially
Silhouette [8]	wavelet	PNN	Classes	
[16]	CSS	RMM	Classes	N/A
[17]	moment	Minimum distance	Types	not cover

Many related work studied of warship classification through many type of data input. Our study would be new and different data input, we studied on use the side view of the distant view images as data input and our descriptive feature method would be invariant under translation, scaling and rotation.

2.3 Silhouette Shape feature to Time series

Usually, image features often used are edges, silhouettes, color or motion. Here, to work with distant view image, we focus on silhouettes because they are similitude and can be relatively robustly from images [18].

Many proposed methods make use of object silhouettes to classify objects. We categorize into three topics: the first is silhouette representation, the second is shape representation and the last is time series, the detail would be further explained.

2.3.1   Silhouette representation

For the representation of silhouette, there are four basic ways: boundaries, regions, moments and structural [19]. Reference [20], categorize silhouette classification approaches are separated into two categories. First is a statistical method, the "extracted feature" from the shape/silhouette. The second method is to transform shape/silhouette into transform-domain (frequency domain) called "transform-based methods". However both methods extract or transform from shape and silhouette. Silhouette is the important information from our distant view image. Our review indicated that shape is the one important feature of silhouette. We studied in depth on the shape representation.

2.3.2   Shape representation

Shape is a useful feature of the distant view and silhouette images, since the other features are not distinct. Shapes related work have been review.

Silhouette image has only two colors in it. The consisting of two colors (or gray values) called binary images. Without loss of generality we call these as 0 and 1 respectively. Summary from [21-25], shape descriptors can be classified to the following properties:

- Region-based and boundary-based (contour-based)
- Global and structural
- Space-domain and transform-domain

The Region-based also use the interior points of the shape, in contrast, boundary-based is considered to be the boundary of the shape. Global methods describe shapes as a whole whereas structural use primitives for different parts of shape. Space-domain approaches work on the image space whereas transform-domain use other spaces, e.g. frequency domain. Classification of shape into region - boundary based and global – structural based can be seen in figure 2.3
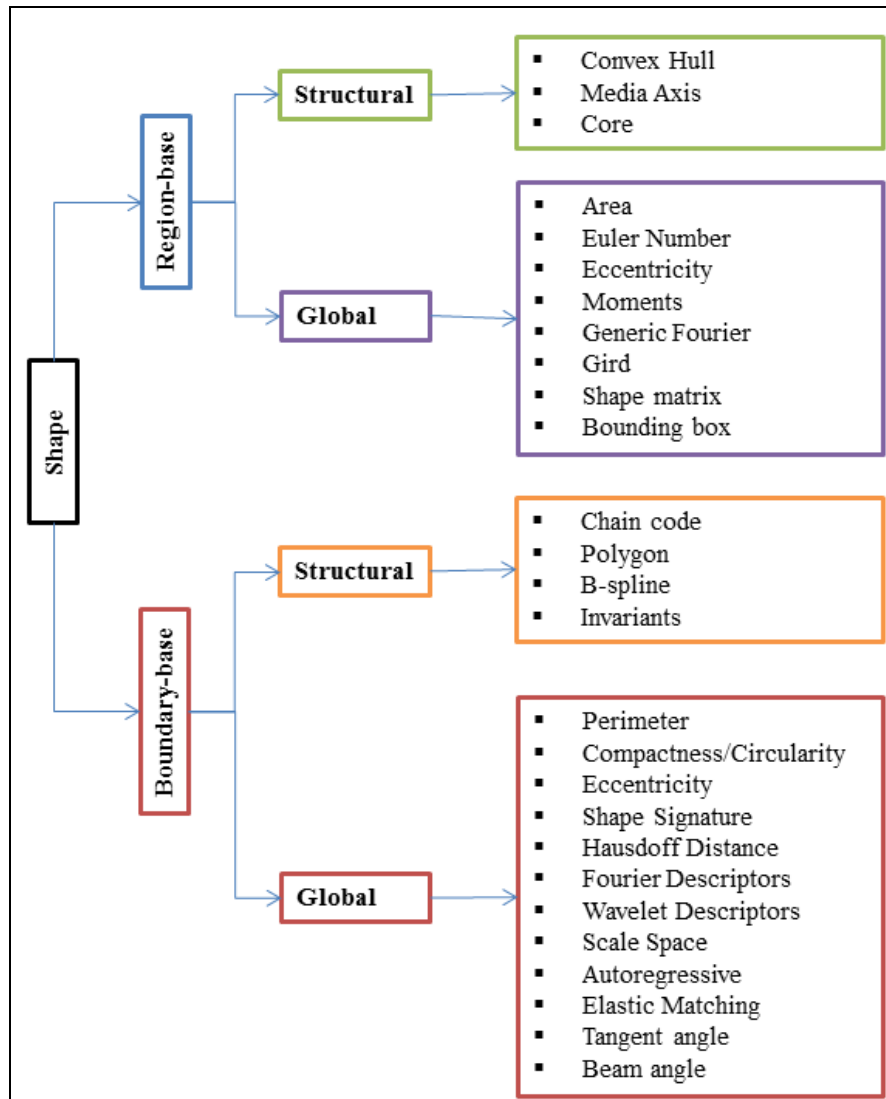
Figure 2.3 Overview of classification of shape descriptors

Boundary-based methods are sensitive to noise and variations. Region-based methods are generally more robust because they use all shape information available and they are able to handle shape defections better. Global methods always contain a trade-off between efficiency and accuracy. The structural methods may be unstable due to high indexing and matching complexity, where the advantage is that partial matching of shapes is possible [26]. However, Summary of [21], [22], [26], [27] and based on our purpose which focuses on the simple and computational complexity (simple and fast) and invariant shape descriptors shown in Table 2.3.

Table 2.3 Shape representation based-on simple and invariant

Descriptor	Simple	Computational complexity	Invariant		
			Translation	Scale	Rotation
Area	✓	✓	✓		✓
Perimeter	✓	✓	✓		✓
Circularity (Compactness)	✓	✓	✓	✓	✓
Eccentricity	✓	✓	✓	✓	✓
Major axis	✓	✓			
Shape signatures	✓	✓			
Shape contexts			✓	✓	✓
Moment			✓	✓	✓
Convex			✓	✓	✓
Tangent angle	✓	✓	✓	✓	✓
Contour curvature			✓	✓	✓
Triangle-area			✓	✓	✓
Beam angle		✓	✓	✓	✓

2.3.2.1 Simple and Computational complexity [22]

Simple and computational complexity properties are very useful for filter to eliminate false hits or combined with other descriptors to decrease the number before more complicated descriptors are used for matching. They are not suitable to be a stand-alone descriptor [26]. These shape descriptors are area, perimeter, circularity (compactness), eccentricity and major axis orientation. However, based on our method that used in Chapter III, area, perimeter and circularity are introduced in this section.

- Area

Area is based on region based. Area is the actual number of all pixels in the region, "…when the boundary point change along the shape boundary, the area of the triangle formed by two successive boundary points and the center of gravity also change. This forms an area function which can be exploited as shape descriptions." [22]. Figure 2.4 shows an example of that let S(n) be the area between the successive boundary points P_n, P_{n+1} and center of gravity G.

(a) Original contour   (b) the area function of (a).
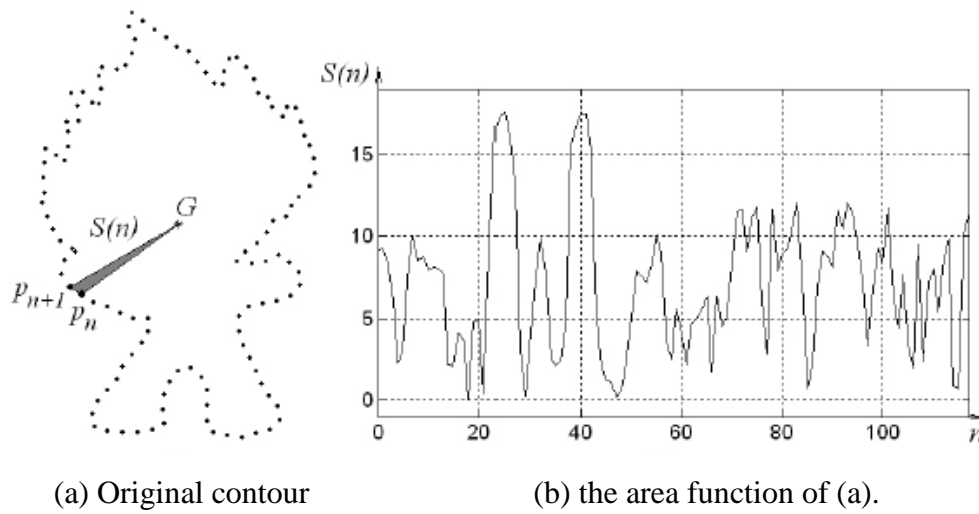
Figure 2.4 Area representation

The area function is linear under affine transform. However, this linearity only work with shape sampled of the same vertices.

- Perimeter and convex perimeter

Perimeter is an important feature of an object. However, boundary-based features such as perimeter which ignores the interior of shapes, this depends on the perimeter or boundary points of the object. The perimeter of an object is given by the integral as follows:

$$T = \int \sqrt{x^2(t) + y^2(t)} dt \tag{1}$$

This perimeter is used for the parametric boundary representation. By the aid of a boundary following algorithm, the object perimeter can be found. The boundary coordinate list by the following equation:

$$T = \sum_{i=1}^{N-1} di \ = \sum_{i=1}^{N-1} |xi - xi + 1| \tag{2}$$
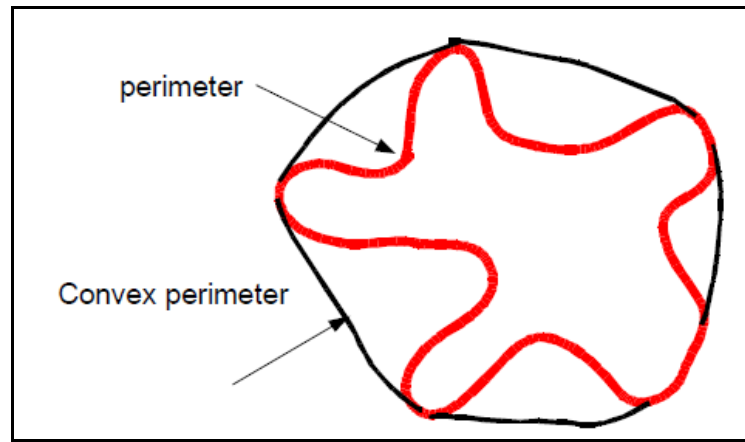
Figure 2.5 Object perimeter and convex perimeter

- Circularity (Compactness)

Circularity or Compactness is the ratio of the area of the object to the area of a circle. The circle is defined by the same center of mass as the object and its radius is defined by the average distance from the center of mass to the perimeter of the object [28]:

$$Compactness = \frac{4\pi \times area}{(perimeter)^2} \tag{3}$$

As a circle is the object with the most compact shape, a circle takes the maximum value of compactness is 1, while a square has the value of $4/\pi$.

Figure 2.6 redrawn from [28], shows different compactness values for different objects.

Low compactness   High compactness
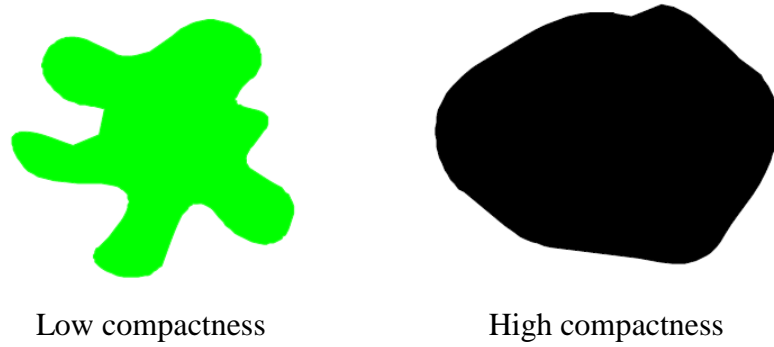
Figure 2.6 Different compactness of object

This feature is motivated by the fact that attached normal growing cells will have a low compactness value.

2.3.2.2 Invariant descriptors

To obtain the translation invariant property, usually defined by relative values. To obtain the scale invariant, normalization is necessary. In order to compensate for orientation changes, shift matching is needed to find the best matching between two shapes. Having regard to occultation, Tangent angle, Contour curvature and Triangle-area descriptor have invariance property. As shown in Table 2.3, Tangent angle is one of invariant and simple, we focused on this.

- Tangent angle [26]

The tangent angle function at a point $P_n(x(n),\ y(n))$ is defined by a tangential direction of a contour at that point :

$$\theta(n) = \theta_n = arctan\frac{y(n)-y(n-w)}{x(n)-x(n-w)} \qquad (4)$$

Since every contour is a digital curve; *w* is a small length or window to calculate the $\theta(n)$ more accurately.

Tangent angle function has two problems. First is noise sensitivity. To decrease the effect of noise, a contour would be filtered by a low-pass filter with appropriate bandwidth before calculating the tangent angle function. The other is discontinuity, due to the fact that the tangent angle function assumes values in a range of length 2π, usually in the interval of $[-\pi, \pi]$ or $[0, 2\pi]$. Therefore, θ_n in general contains discontinuities of size 2π. To overcome the discontinuity problem, function φn is defined as the different of angle between the tangent at any point P_n and the next point P_{n+1} along the boundary curve [26]:

$$\varphi(n) = [\theta(n+1) - \theta(n)] \qquad\qquad (5)$$

The other method based on tangent angle is called tangent space representation. "A digital curve C simplified by polygon evolution is represented in the tangent space by the graph of a step function, where the x-axis represents the arc length coordinates of points in C and the y-axis represents the direction of the line segments in the decomposition of C." [26].

Figure 2.7 shows an example of a digital curve and its step function representation in the tangent space.
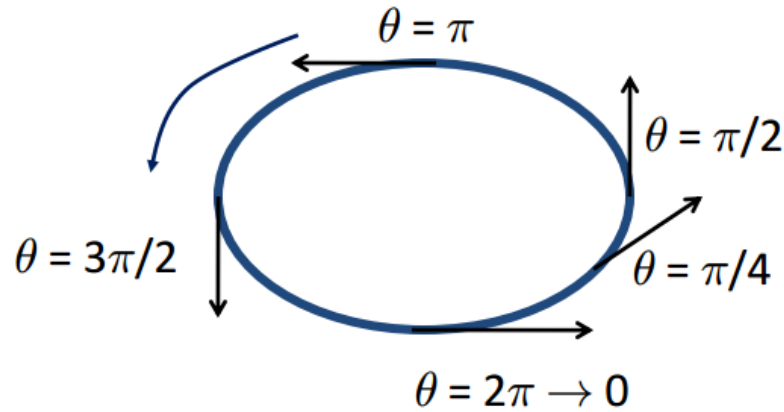
Figure 2.7 Tangent angle

Silhouettes and shapes are the most important features for classification. Reference [27] gave a short list of desirable shape descriptor properties:

- Robustness: the degree of sensitivity to structural defects or random thermal noise

- Invariance: the ability to remain invariant under certain mathematical transformations, scaling and translations. Additionally, possible invariant under rotation and mirroring could occur.

- Efficiency: the computational effort and memory costs are required.

- Comparability: the ease of matching.

Reference [24] compared region-based to boundary-based. Boundary-based are sensitive to noise and variations and not always available. Region-based are generally more robust because they used all shape information available.

However, global methods always contain a trade-off between accuracy and efficiency. Many study discussed the methods as shown in our review. Among them, some are invariant under translation, scaling and rotation in feature extraction step, but some are invariant in measurement step. Some need to calculate and turn back the rotated object before taking measurements.

One of our purposes is to extract the feature from distant view images of warship that is invariant under translation, scaling and rotation with ease and using less computation. Hence, we used invariant and easy feature extraction boundary-based, the tangent-angle based. However, simple and fast process as the circularity (compactness) from region-based cannot use for identify the object but useful for data filtering.

The output from tangent-angle based is the set of angles that similarity to time series called "pseudo-time series". Next, the time series would be discussion.

2.3.3   Time series [24, 29-30]

A time series is a collection of observations made chronologically. The characteristic of time series is numerical that continuous in nature. Nature of time series data includes: large in data size, high in dimension and continuous values [29].

"Increasing use of time series data has initiated a great deal of research and development attempts in the field of data mining." [29]. In the context of time series data mining, the fundamental problem is how to represent the time series data. The common approaches are to transform the time series to other format for dimension reduction and to similarity measure [29].

Two key aspects for achieving effectiveness and efficiency, when managing time series data are representation methods and similarity measures [30].

- Time series representation and indexing

One of the main reasons of time series representation and indexing is to reduce the dimension (the number of data point) of original data.

The simplest method perhaps is sampling [29] that has drawback of distorting the shape of sampled/compressed time series, if the sampling rate is too low.

An enhanced method is called Piecewise Aggregate Approximation (PAA), this method use the average (mean) value of each segment to represent the corresponding set of data points. With time series $P = (p_1,\ldots,p_m)$ and n is the dimension after dimensionality reduction as shown in Figure 2.8.
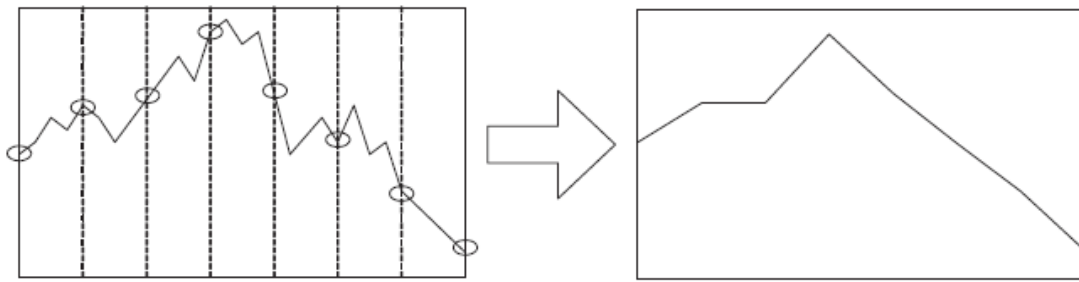
(a) Dimensionality reduction by sampling.
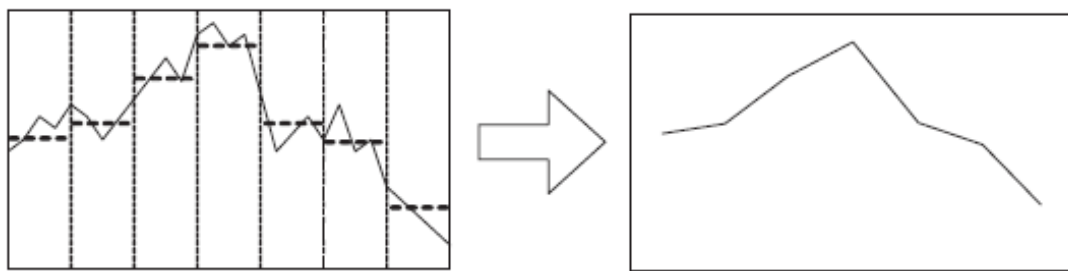
(b) Dimensionality reduction by PAA.
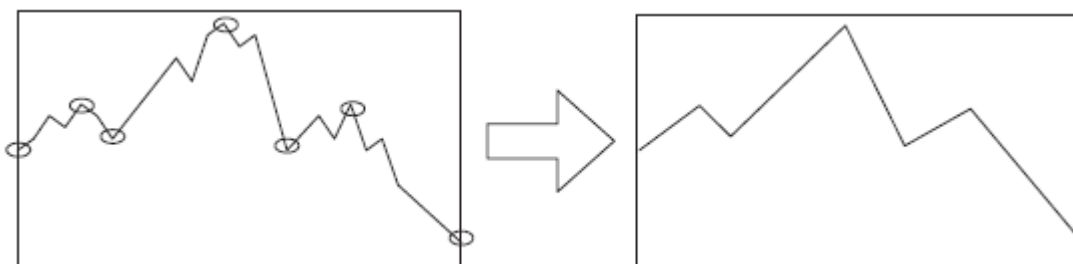
(c) On the right is compression by data point importance,

on the left is PIPs of the right.

Figure 2.8 Dimensionality reductions by sampling (a), PAA (b) and PIPs (c) [29].

The PAA is fix in length of data, but an extended of PAA is an adaptive piecewise constant approximation (APCA), which the length of each segment is not fixed as PAA, adaptive to the shape of the series. Furthermore, "… reducing the dimension by preserving the salient points are a promising method. These points are recalled as perceptually important points (PIP)." [29]. The PIP used for pattern matching of technical patterns in financial applications. With the time series P, there are n data points: P_1, P_2…, P_n. All the data points in P can be reordered by its

importance by going through the PIP identification process. The first data point P1 and the last data point Pn in the time series are the first and two PIPs, respectively. The next PIP that is found will be the point in P with maximum distance to the first two PIPs. The fourth PIP that is found will be the point in P with maximum vertical distance to the line joining its two adjacent PIPs, either in between the first and second PIPs or in between the second and the last PIPs. The PIP location process continues until all the points in Pare attached to are ordered list L or the required number of PIPs is reached [29].

Figure 2.8 (c) shown that the seven PIPs identified   from sample time series (a) and (b).

Another common family of time series representation approaches converts the numeric time series to symbolic format. That is, first discretizing the time series into segments called PAA, then converting each segment of PAA into a symbol called Symbolic Aggregate approximation (SAX) that based on PAA.

To sum up for a given index structure, the efficiency of indexing depends only on the precision of the approximation in the reduced dimensionality space. However, "…in choosing a dimensionality reduction technique, we cannot simply choose an arbitrary compression algorithm." [29].

- Time series similarity measures

For similarity measures of time series, given two time series T1 and T2, a similarity function *Dist* calculates the distance between the two time series, denoted by *Dist(T1,T2)*. We refer to distance measures that compare the i_{th} point of one time series to the i_{th} point of another. Reference [30] has reviewed the 9 similarity measures evaluated: Euclidean (ED), Dynamic Time Warping (DTW), Longest Common SubSequence (LCSS), Edit Sequence on Real Sequence (EDR), Swale, Edit Distance with Real Penalty (ERP), Threshold query based similarity search (TQuEST) and Spatial Assembling Distance (SpADe). The summary was shown in Table 2.4.

Table 2.4 Summary of Similarity Measures [30-31]

Distance function	Advantages	Disadvantages
Euclidean/ Manhattan	Complexity Easy to implement Indexable Parameter-free	Sensitive to noise Misalignments in time Shifting
DTW	Allow to "stretched"	Cost for computation
LCSS	Allow some unmatch Consideration on the outliers	Based on symbolic
EDR	Penalties of gaps	N/A
SpADe	N/A	Requires many parameters

By comparing the performance and accuracy, EDR, LCSS and ERP are very close to DTW, while TQuEST is worse than ED and DTW in some data set. Swale is clearly superior to ED and almost as accurate when compared to LCSS. The accuracy of SpADe is close to ED but inferior to DTW.

However, according to the unique behavior of time series data [29], there is no clear evidence that one method exists on similarity measure is superior to others [30].

- Classification for time series

Classification for time series has been studied. There are several classifications that could be used such as k-nearest neighbor (k-NN), Bayesian network, Neural Network (NN), Decision Trees, Fuzzy Logic, and Support Vector Machine (SVM). Each of classification method can be used in various situations as needed where one tends to be useful while the other may not and vice-versa [32]. However, on comparison of classification [21], with cross-validation, decision tree, SVM and k-NN show good performance, however k-NN is better in noise data.

K-NN is instance-based learning or lazy-learning. "The principle is based on the instances within a dataset; generally exist in close proximity to other instances that have similar properties." [33].

The power of k-NN has been demonstrated in a number of real domains, but there are some reservations about the usefulness, such as [33]:

i)   they have large storage requirements,

ii)   they are sensitive to the choice of the similarity function that is used to compare instances,

iii)   they lack principle way in choosing k value and the major disadvantage is their lengthy computational time for classification.

SVM are the new supervised machine learning. They can operate correctly even if the designer does not know exactly the features of the transformed feature space. However, the SVM are binary, in case of multi-class problem, one must reduce the problem to a set of multiple binary classification problems and require large sample size. Generally, SVM and ANN tend to perform much better when dealing with multi-dimensions and continuous features. Summary of classifiers are shown below:

Table 2.5 Summary of Classifiers [21, 32-34]

Classifier	Training time	Advantages	Disadvantages
SVM	Slow	-nonlinear	-need large data size
ANN	Slow	-accuracy	-hidden layer
k-NN	0	-noise -ease to implement	-computational complexity
Bayes	Fast	-understood -require little storage	-not suitable for many features
Trees	Fast	-interpretable -computational cheap -easy to implement	-require more data

During our reviews, there is as no clear picture of which method is the best classifier. However reference [32-34] show that k-NN has the best for speed of learning, to dealing with danger of over fitting and attempts for incremental learning and [19] has been proven 1-NN with DTW that it is the best technique to produce the maximum accurate result.

Based on our purpose and method, we found that PAA and SAX have advantage in term of dimensionality reduction technique but SAX has disadvantage that the original data have to turn to symbolic.

In our experimental, we used 1-NN, PAA and compared between ED and DTW for similarity measurement performance. However, the advantage and reason would be discussed.

2.4 Contour Tracing

Contour tracing is one of basic preprocessing techniques that work on digital images, the goal of contour tracing is to extract information from their general shape. When the contour is extracted, its different characteristics will be examined and used as features which will later be used in shape matching. Therefore, correct extraction of the contour produces more accurate features that provide correctly classifying of a shape.

In order to find an external contour at a given pixel S, at this pixel, we first execute Tracer. If Tracer identifies S as an isolated pixel, we would reach the end of Contour Tracing. Otherwise, Tracer will give an output of the next contour point of S., named this point T. We then continue to execute tracer to find the next contour point of T. The process is proceeding until the following two conditions found:

(i)   Tracer outputs S again, and

(ii) The next contour point of S is T again

Then the process would stop only when both conditions above are met [35].
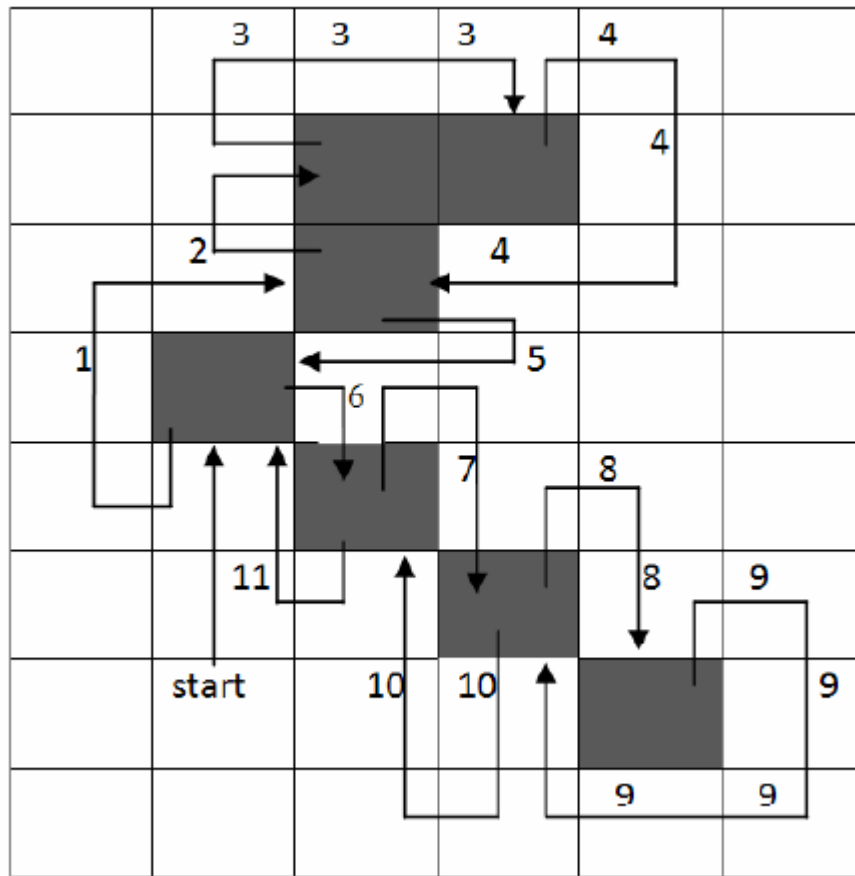
Figure 2.9 Working of Moore's Neighbor tracing algorithm [35]

Moore Neighborhood of a pixel, P, is a set of 8 pixels which share a vertex or an edge with that pixel.

The basic idea is that when the current pixel p is black, the Moore neighborhood of p is examined in clockwise direction, starting with the pixel from which p was entered and advancing pixel by pixel until a new black pixel in P is encountered. The algorithm terminates when the start pixel is visited for second time. The black pixel walked over will be the contour of the pattern. "… The main weakness of Moore Neighbor tracing lies in the choice of stopping criteria i.e. visiting the start pixel for second time. If the algorithm depends on this criterion all the time it fails to trace contour of large family of patterns. Mostly, it uses stopping criterion i.e.

i. Stop after visiting the start pixel n times, where n is at least 2, or

ii. Stop after visiting the start pixel second time." [35].

Figure 2.9 demonstrates the working of Moore Neighbor contour tracing algorithm for an input pattern. The line number indicates the iteration number of traversal.

The output of this contour tracing technique is an array of boundary coordinates of the image. This coordinate set is used for our feature extraction process by give this array to tangent function and different of angle. The Piecewise Aggregate Approximation technique is used for dimension reduction.

2.5　Piecewise Aggregate Approximation (PAA)

To speed up the computation, reference [36] reduces the data from n dimensions to N dimensions by dividing the time series into N equal-sized 'frames'. The mean value of the data that falls within a frame is calculated, and a vector of these values becomes the reduced data representation. The transformation produces a piecewise constant approximation of the original sequence, hence the name, Piecewise Aggregate Approximation (PAA). Reference [36] suggests approximating a time series by dividing it into equal-length segments and recording the mean value of the data points that fall within the segment and speeds up of DTW by modification to PAA with no loss of accuracy.

This simple technique is surprisingly competitive with the more sophisticated transformation used in [37]. Reference [38] proposed that also propose PAA can reduce the computational time and in turn increase the number of DTW calculations; the proposed PAA lower-bound estimate is calculated to enable the increase in speed of the overall DTW-k-NN search by 28%.

To demonstrate this technique, Figure 2.10 (a) reduced dimension from 250 to 16 and Figure 2.10 (b) compared the dimension reduction between original of 60 to new dimension of 10.
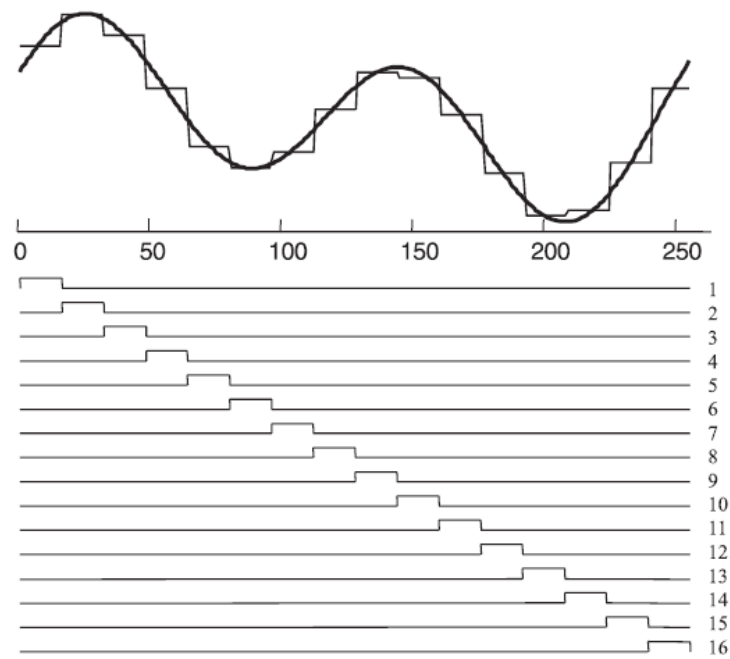
(a)
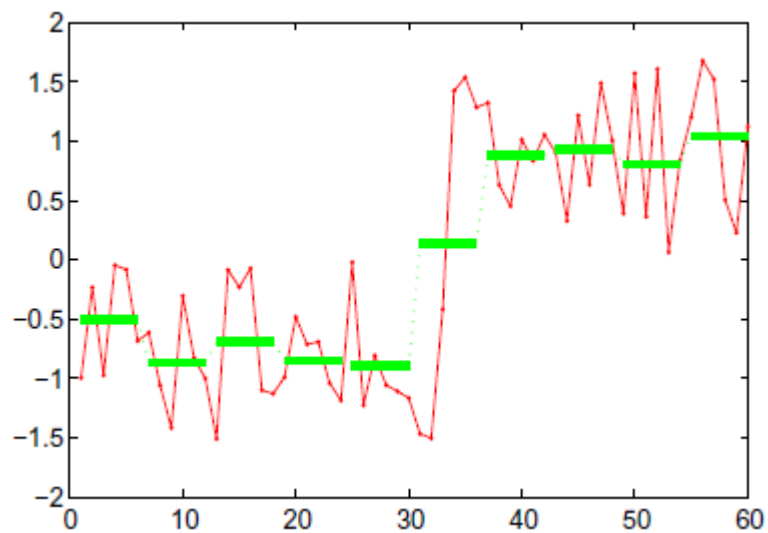
(b)

Figure 2.10 The PAA representations can be readily visualized as an attempt to model
a sequence with a linear combination of box basis functions [31].

SAX (Symbolic Aggregate approXimation) is a symbolic representation of time series. SAX allows a time series of arbitrary length n to be reduced to a string of arbitrary length w.
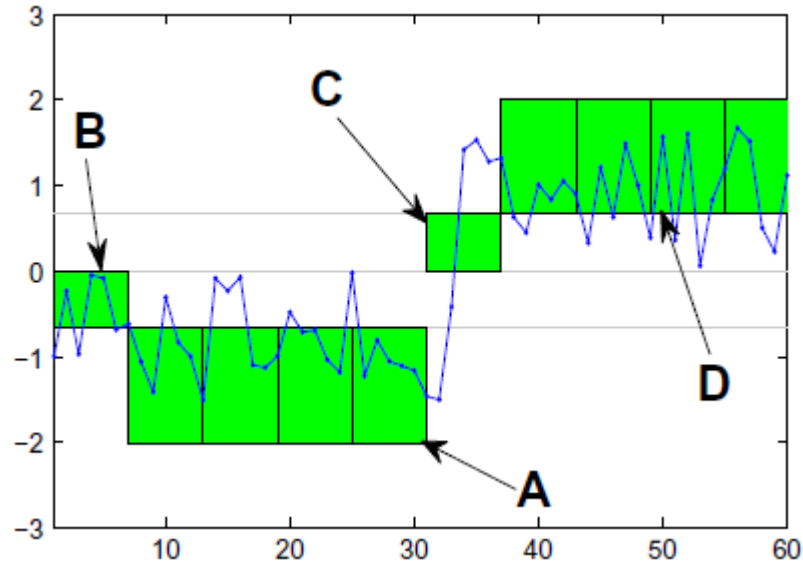
Figure 2.11 The SAX of PAA calculated from Figure 2.10 [31]

2.6   Dynamic Time Warping (DTW)

The dynamic time warping (DTW) algorithm is a well-known algorithm in many areas of study. Introduced as an application for speech recognition, it is currently used in many areas, including data mining and time series [39].

DTW may be considered simply as a tool to measure the dissimilarities between two time series after aligning them.

Suppose we have two time series Q and C, of length p and m, respectively, where:

$$Q = q_1, q_2, \ldots q_p \tag{6}$$

$$C = c_1, c_2, \ldots c_m \tag{7}$$

In order to compare the two different sequences Q and C the local distance measure is used.

The algorithm starts by building a distance matrix (p-by-m) representing all pairwise distances between C and Q. This distance matrix is called the local cost matrix.

Once the local cost matrix has been built, the algorithm is used to determine the alignment path that intersects the low-cost areas or "valleys" on the cost matrix.
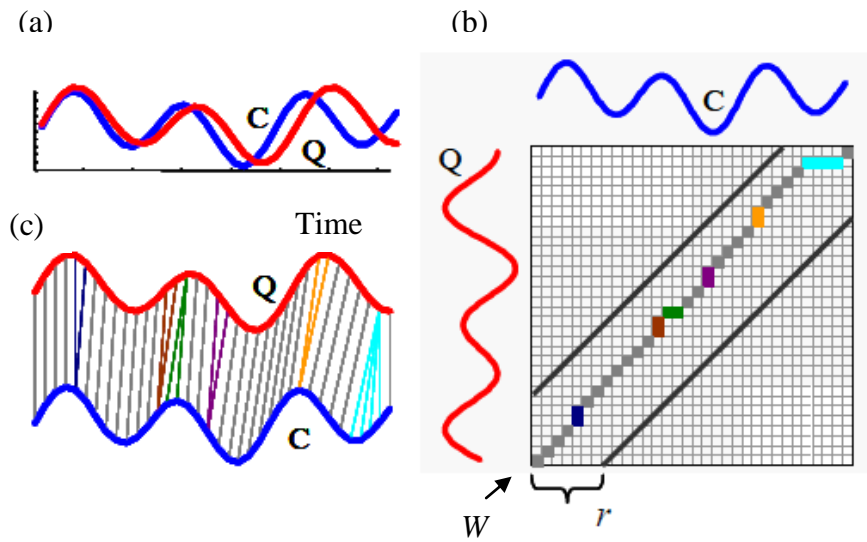
Figure 2.12 Two similar time series Q and C (a). (b) A warping matrix and search for the optimal warping path (solid squares). (c) The resulting alignment [40].

Figure 2.12 (a, c) shows two time series sequences which are similar but out of phase. To align the sequences, we constructed a warping matrix and searched for the optimal warping path, represented by solid squares. A band with width "r" constrains the warping (b).

The warping path "W" is a contiguous set of matrix elements that defines the mapping between Q and C. The k_{th} elements of W are defined as $w_k = (i, j)_k$ as below:

$$W = w_1, w_2, ...,w_k,...,w_K \quad max(m, p) \leq K \leq m+p-1 \tag{8}$$

The warping path must satisfy several constraints [40]:

-Boundary conditions: $w_1 = (1, 1)$ and $w_k = (p, m)$, requiring the warping path to start and finish in diagonally opposite corners;

-Continuity: Given $w_k = (a, b)$ then $w_{k-1} = (a', b')$ where $a - a' \leq 1$ and $b - b' \leq 1$. This restricts the allowable steps in the warping path to adjacent cells;

-Monotonicity: Given $w_k = (a, b)$ then $w_{k-1} = (a', b')$ where $a - a' \geq 0$ and $b - b' \geq 0$.
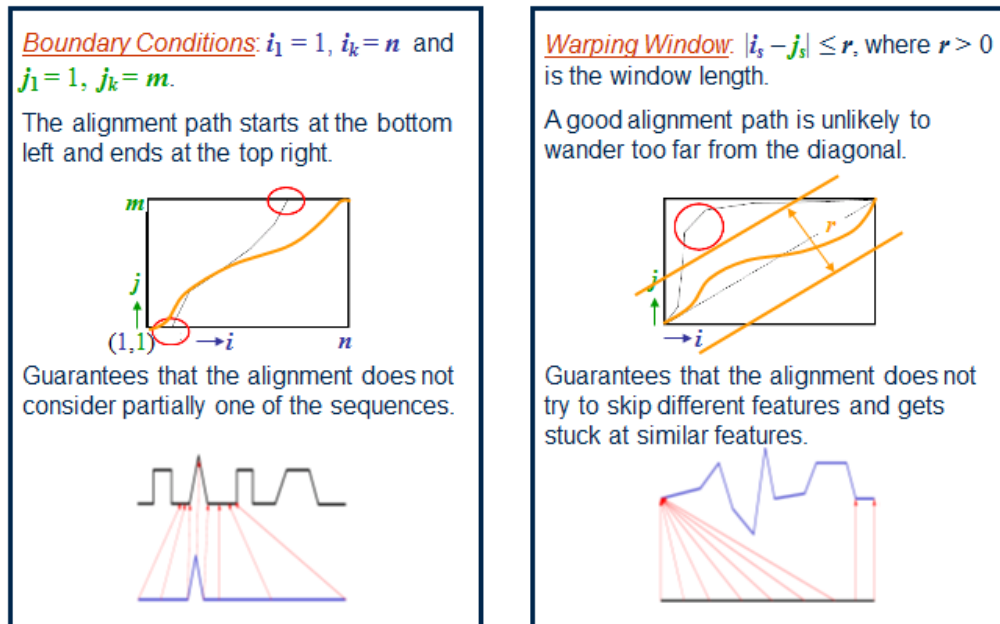
Figure 2.13 Constraints of Dynamic Time Warping
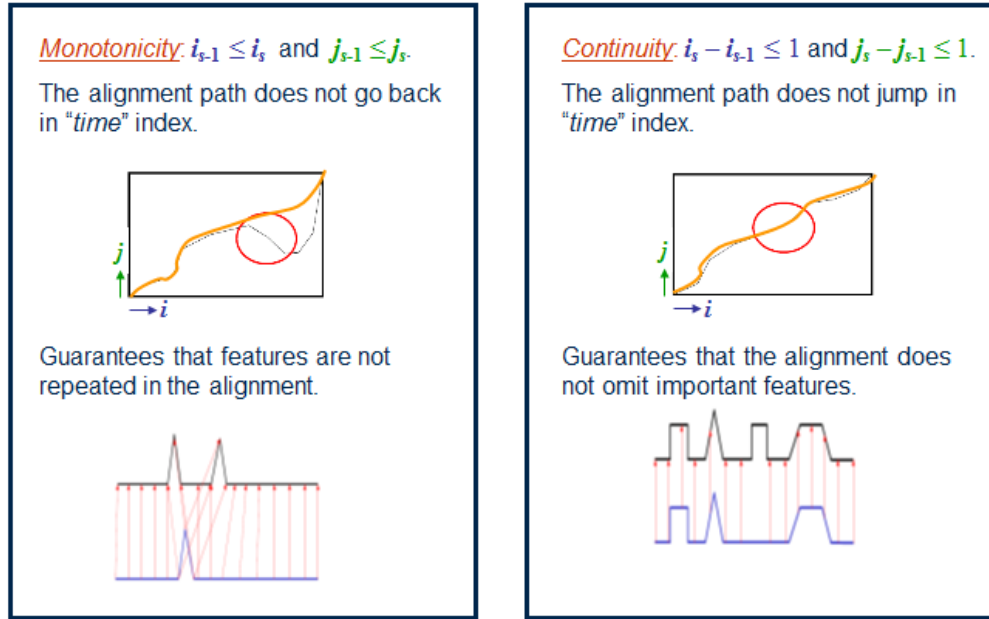
Figure 2.13 Constraints of Dynamic Time Warping (cont.)

This forces the points in W to be monotonically spaced in time. We are interested in the path that minimizes the warping cost:

$$DTW(Q,C) = \min\left\{\sqrt{\sum_{k-1}^{k} w_k}\right\} \qquad (9)$$

This path can be found using dynamic programming to evaluate the following recurrence which defines the cumulative distance $\gamma(i, j)$ as the distance $d(i, j)$ found in the current cell and the minimum of the cumulative distances of the adjacent elements:

$$\gamma(i, j) = d(qi, cj) + min\{ \gamma(i-1, j-1), \gamma(i-1, j), \gamma(i, j-1) \} \qquad (10)$$

The time cost of building this matrix is O(pm). In order to improve performance and customize the sensitivity of the naive DTW algorithm, various modifications are proposed. The major modifications include step size conditions, step weighting, and global path constraints.

To prove this, we followed the naive DTW as shown in [39] and 1-NN using dynamic time warping (1NN-DTW). This seems to be the best approach for time series classification shown in [40] and [41].

The algorithm of DTW:

Algorithm: *AccumulatedCostMatrix(X, Y)* [39]

```
 1: n ← |X|
 2: m ← |Y|
 3: dtw[] ← new [n × m]
 4: dtw(0, 0) ← 0
 5: for i = 1; i ≤ n; j + + do
 6:     dtw(i, 1) ← dtw(i − 1, 1) + c(i, 1)
 7: end for
 8: for j = 1; j ≤ m; j + + do
 9:     dtw(1, j) ← dtw(1, j − 1) + c(1, j)
10: end for
11: for i = 1; i ≤ n; j + + do
12:     for j = 1; j ≤ m; j + + do
13:         dtw(i, j) ← c(i, j)+min {dtw(i − 1, j); dtw(i, j − 1); dtw(i − 1, j − 1)}
14:     end for
15: end for
16: return  dtw
```

Algorithm : *OptimalWarpingPath(dtw)* [39]

```
 1: path[] ← new array
 2: i = rows(dtw)
 3: j = columns(dtw)
 4: while (i > 1) & (j > 1) do
 5:    if i == 1 then
 6:       j = j − 1
 7:    else if j == 1 then
 8:       i = i − 1
 9:    else
10:       if dtw(i−1, j) == min {dtw(i − 1, j); dtw(i, j − 1); dtw(i − 1, j − 1)}
          then
11:          i = i − 1
12:       else if dtw(i, j−1) == min {dtw(i − 1, j); dtw(i, j − 1); dtw(i − 1, j − 1)}
          then
13:          j = j − 1
14:       else
15:          i = i − 1; j = j − 1
16:       end if
17:       path.add((i, j))
18:    end if
19: end while
20: return path
```

"In reality, DTW may not give the best mapping according to our need because it will try its best to find the minimum distance. It may generate the unwanted path. For example, without global constraint, DTW will find its optimal mapping." [40].

Sakoe-Chiba band (S-C band), shown in Figure 2.14 (b), is one of the simplest and most popular global constraints, originally introduced to be used for speech community. The width of this global constraint is generally set to be at 10% of time series length [40]. However, the different sizes of the band can be used for a more accurate classification. Therefore, we need to test all possible widths of the global constraint so that the best width could be discovered. An evaluation function is needed to justify the selection. We commonly use accuracy metric (a training accuracy) to be the measurement. An algorithm in finding the best warping window for S-C band by decrementing the band size by 1% in each step, this function receives a set of data *T* as an input, and the best warping window (*best_band*) as an output. Note that if an

evaluation value is equal to the best evaluation value, we prefer the smaller warping window size.

Algorithm: Finding the best warping window [37].

Function $[best\_band]$ = best_warping(T)	
1	$best\_evaluate$ = Negative_Infinite;
2	**for** $(k = 100$ to $0)$
3	$band_k$ = S-C band at $k\%$ width;
4	$evaluate$ = evaluate$(band_k)$;
5	**if** $(evaluate >= best\_evaluate)$
6	$best\_evaluate$ = evaluate;
7	$best\_band$ = $band_k$
8	**endif**
9	**endfor**

Ratanamahatana-Keogh band (R-K band) is one of a general model of a global constraint specified by a one-dimensional array R, i.e., $R = r_1, r_2, ..., r_n$ where n is the length of time series, and r_i is the height above the diagonal in y direction and the width to the right of the diagonal in x direction. Each r_i value is arbitrary, therefore R-K band is also an arbitrary-shape global constraint, as shown in Figure 2.14 (a). Note that when $r_i = 0$, where $1 < i \leq n$, this R-K band represents the Euclidean distance, and when $r_i = n, 1 < i \leq n$, this R-K band represents the original DTW distance with no global constraint. The R-K band is also able to represent the S-C band by giving all $r_i = c$, where c is the width of a global constraint. Moreover, the R-K band is a multi- band model which can effectively be used to represent one band for each class of data [37].
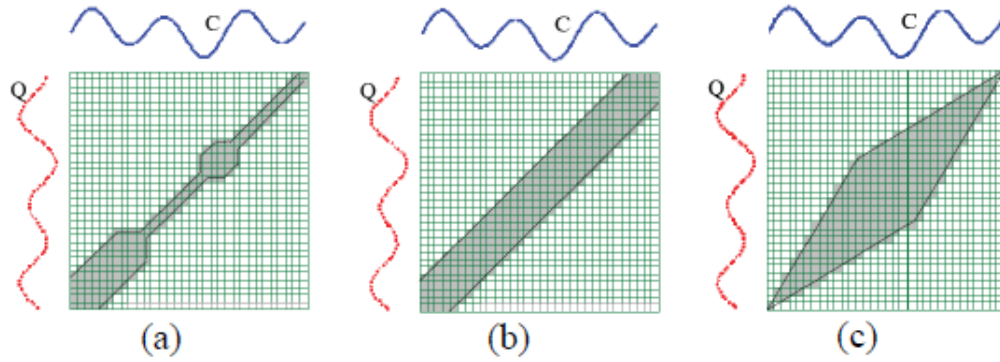
Figure 2.14 Global constraint examples of (a) R-K band, (b) S-C band,

and (c) Itakura Parallelogram [42]

2.7 k-Nearest Neighbor (k-NN)

Supervised learning is the most fundamental task in machine learning. In supervised learning, we have training examples and test examples. A training example is an ordered pair (x, y) where x is an instance and y is a label. A test example is an instance x with an unknown label. The goal is to predict labels for test examples [43]. One example for an instance-based learning algorithm is the k-Nearest Neighbor (k-NN) algorithm. It uses the k-nearest neighbors to make the decision of class attribution directly from the training instances themselves. The decision for attaching the sample in question to one of the several classes is based on the majority vote of its k-nearest neighbors. An odd number should be chosen for k to allow for a definite majority vote [44]. The k-NN method is perhaps the simplest of all algorithms for predicting the class of a test example. "There are two major design choices to make; the value of "k", and while distance function to use. In order to avoid ties, the most common choice for k is a small odd integer, for example k = 3. Ties can also arise when two distance values are the same." [43].

Usually, Euclidean distance is used for the distance function. The Euclidean distance between x_q and x_i is calculated as follows:

$$dist\left(X_q, X_i\right) = \sqrt{\left(\sum_{k=1}^{n}\left(\left(X_{q,k}\right) - \left(X_{i,k}\right)\right)\right)^2} \qquad (11)$$

Some papers used k-NN with DTW for time-series classification: [40], [41] and [45]. Hence, for our experiment, we used 1-NN and DTW for the distance function instead of Euclidean distance.

2.8 Image processing [46]

The basic process in digital images that usually for pre-processing; the brightness variation by using its histogram, thresholding techniques that turn an image from gray color to binary images and the statistical operations to reduce noise. We focused on these basic techniques.

A computer image is a matrix (a two-dimensional array) of pixels. "…The value of each pixel is proportional to the brightness of the corresponding point in the scene; The matrix of pixels, the image, is usually square and we shall describe an image as $N \times N$ m-bit pixels where N is the number of points along the axes and m controls the number of brightness values." [46]. Using m bits gives a range of 2^m values, ranging from 0 to $2^m - 1$ [46].
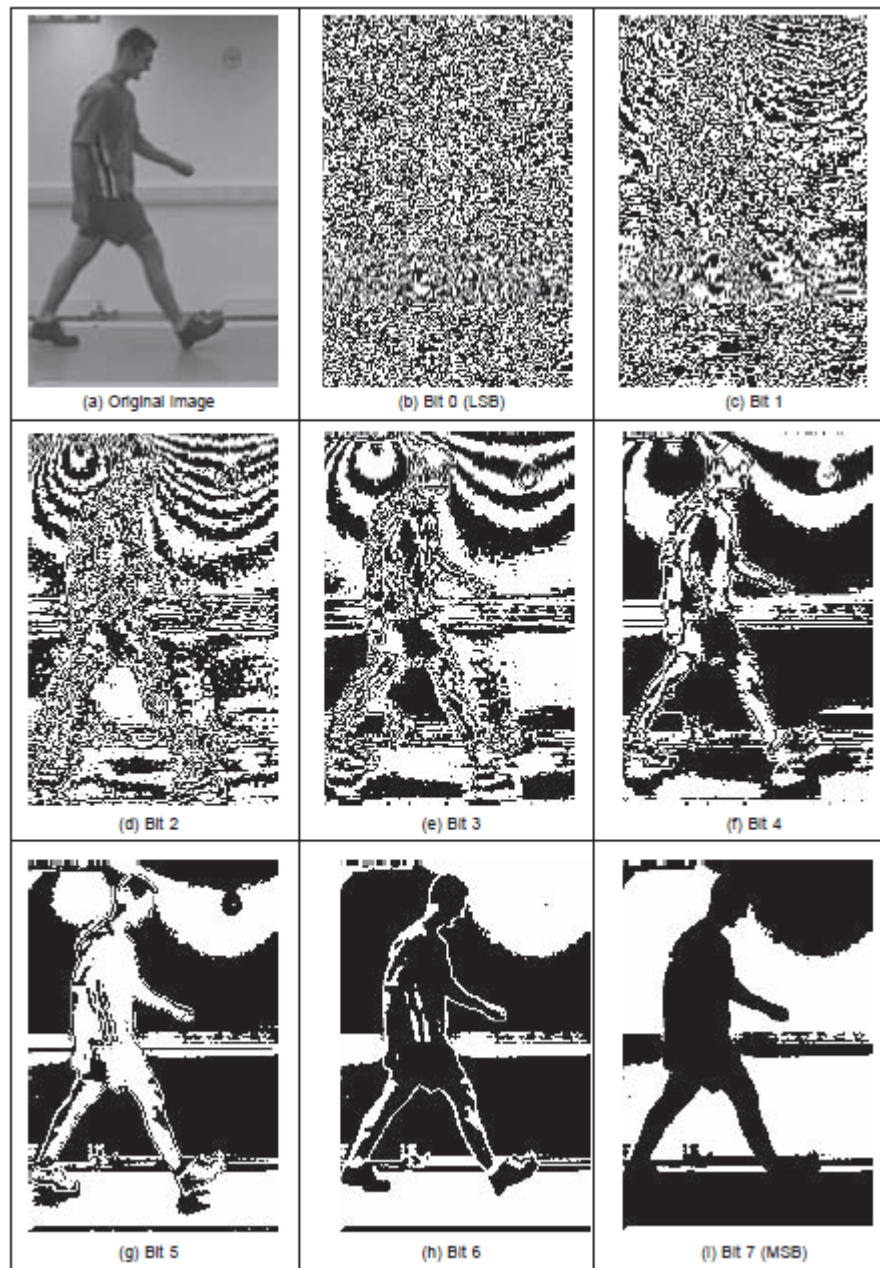
Figure 2.15 Decomposing an image into its bits [46]

"… If m is 8, this gives brightness levels ranging between 0 and 255, which are usually displayed as black and white, respectively, with shades of grey in between, as seen in the grey-scale image of an image in Figure 2.15(a). Smaller values of m give fewer available levels reducing the available contrast in an image." [46]

The relative influence of the 8 bits is shown in the image of the walking subject in Figure 2.15. Here, the least significant bit, bit 0 (Figure 2.15(b)), carries the least information. The most information is carried by the most significant bit, bit 7 (Figure 2.15(i)).

We would consider the processing of grey level images only since they contain enough information to perform feature extraction and image analysis. Should the image be originally color, we will consider processing its luminance only, often computed in a standard way. In any case, the amount of memory used is always related to the image size.

2.8.1   Preprocessing

The input images need to pre-process before main process of our method, by using the thresholding, the main object and the background could separate.

"… the last point operator of major interest is called thresholding. This operator selects pixels which have a particular value, or are within a specified range. It can be used to find objects within a picture if their brightness level is known. This implies that the object's brightness must be known as well." [46]. There are two main forms for thresholding: uniform and adaptive. In uniform thresholding, pixels above a specified level are set to white; those below the specified level are set to black [46].

Figure 2.16 (a) is the original ship image and Figure 2.16 (b) shows a threshold image where all pixels above 0.6 brightness levels are set to white, and those below are set to black.

By this process, the parts of ship body are separated from the background; the bright areas are separated from the dark. This can therefore provide a way of isolating points of interest.
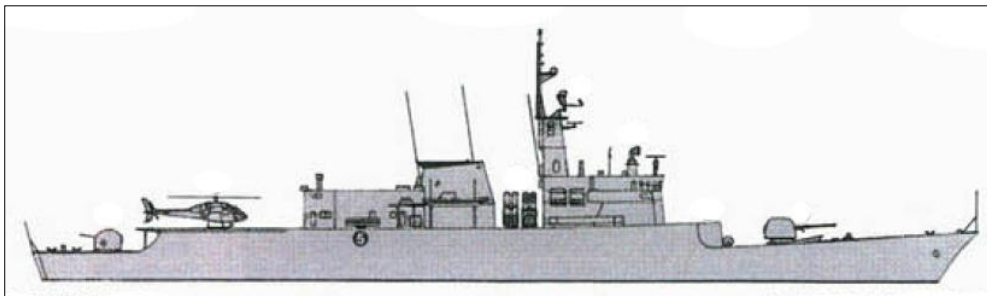
(a) Original image
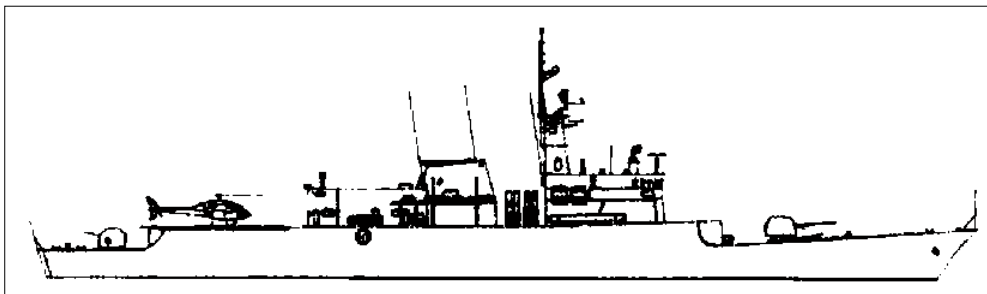
(b) Threshold at level 0.6

Figure 2.16 Thresholding the ship image

The selection by Otsu is automatic, as opposed to manual and this can be to application advantage in automated vision.
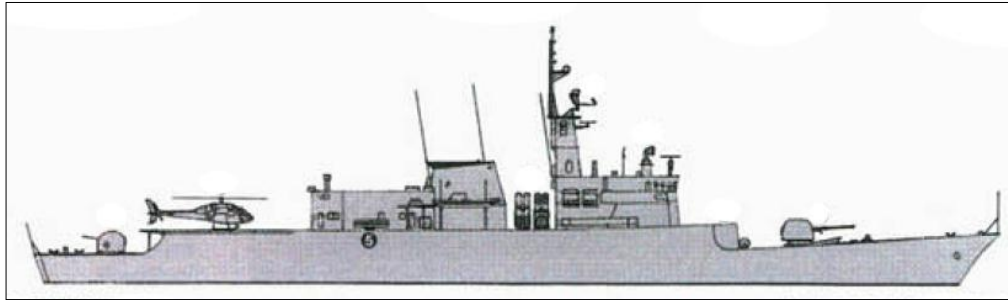
(a) Original image
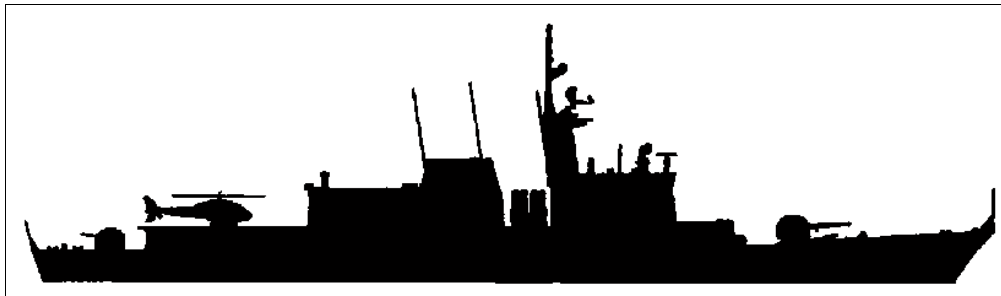
(b) Thresholding by Otsu

Figure 2.17 Automatic thresholding the ship image

Consider, for example, the need to isolate the ship figure in Figure 2.17(a). This can be performed automatically by Otsu as shown in Figure 2.17(b). It is easy to remove the isolated points of interest.

2.8.2 Histograms

The histogram provides a natural bridge between images and a probabilistic description. The basis used of the normalized histogram where the number of points at each level is divided by the total number of points in the image. A histogram of an image provides the frequency of the brightness and darkness value in the image, the histogram of an image with gray-levels is represented by an array of elements [46].

(a) An original image
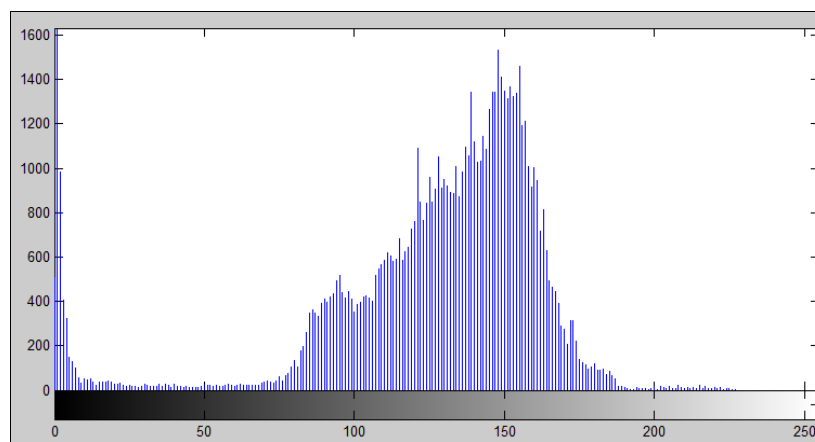
(b) Histogram of image (a)

Figure 2.18 Histogram, Original images (a) and its brightness histogram (b).

Computing the brightness histogram [46]:

1. Assign zero values to all elements of the array h_f.

2. For all pixels (x,y) of the image f, increment $h_f(f(x,y))$ by 1 .

We might want to find a first-order probability function to indicate the probability that pixel (x, y) has brightness. Dependence on the position of the pixel is not of interest in the histogram; a density function is of interest and the brightness histogram is its estimate. The histogram is often displayed in a bar graph as shown in Figure 2.18 (b). The histogram is usually the only global information about the image which is available, and use when finding optimal illumination conditions for capturing an image, gray-scale transformations, and image segmentation to objects and background.

2.8.3 Convolution

Image smoothing is the pre-processing methods that used to smooth the image noise or boundary of image. By calculated the new value based on averaging of original value of the image. This is illustrated in Figure 2.19 where a new image is calculated from an original one, by template convolution. "…The calculation obtained by template convolution for the center pixel of the template in the original image becomes the point in the output image. When the template reaches the end of a line, it is repositioned at the start of the next line. For a 3 x 3 neighborhoods, nine weighting coefficients w_t are applied to points in the original image to calculate a point in the new image. To calculate the value in new image N at point with co-ordinates x, y…" [46], the template in Figure 2.20 operates on an original image O according to:

$$N_{x,y} = \begin{matrix} w_0 + O_{x-1,y-1} + w_1 + O_{x,y-1} + w_2 + O_{x+1,y-1} + \\ w_3 + O_{x-1,y} + w_4 + O_{x,y} + w_5 + O_{x+1,y} + \\ w_6 + O_{x-1,y+1} + w_7 + O_{x,y+1} + w_8 + O_{x+1,y+1} + \end{matrix} \quad \forall_{x,y} \in 2, N-1 \quad (12)$$
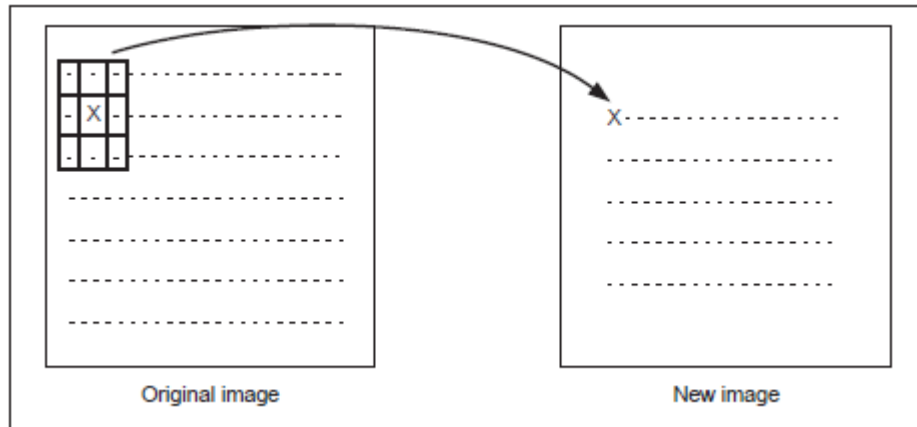
Figure 2.19 Template convolution process [46]

Figure 2.20 Template 3 x 3 and weighting coefficients [46]

Note that we cannot ascribe values to the image's borders. That is because "…when we place the template at the border, parts of the template fall outside the image and we have no information from which to calculate the new pixel value. The width of the border equals half the size of the template." [46], to calculate values for the border pixels, we now have three choices: [46].

1. Setting the border to black;

2. Assume that the image replicates to infinity along both dimensions and calculate new values by cyclic shift from the far border; or

3. Calculated the pixel value from a smaller area.

The template is convolved at each picture point by generating a running summation of the pixel values within the template's window multiplied by the respective template weighting coefficient. Finally, the resulting image is normalized to ensure that the brightness levels are occupied appropriately.

Hence, we used all reviewed techniques and focused on using PAA for dimension reduction, the distance function were ED and DTW that provided data input to 1-NN classifier detail would be discussed in Chapter III.

CHAPTER III
MATERIALS AND METHODS

In this chapter we will explain; materials used, how we collect and generated the data, general processing and our methods step by step.

3.1 Materials

3.1.1 Hardware
Personal Computer

- CPU   :   AMD Dual-Core A4-3300M
- RAM   :   4 GB
- Hard Disk   :   500 GB
- Monitor   :   Acer

3.1.2 Software

- Operation System   :   Windows 7
- Programming Language   :   MATLAB
- Statistical Analysis   :   SPSS
- Graphics   :   PHOTOSHOP
- Documentation   :   MS Word

3.2 Data and Preprocessing

For our experiment, we used silhouettes images of warship from Jane's Fighting Ships 2010 – 2011[47] and Jane's Warship Recognition Guide [48] as input data images. Preprocessing removed the background from the images and smoothing the boundary by using convolution technique.

3.3 General Processing

Figure 3.1 shows the general concept of an algorithm for warship classification.
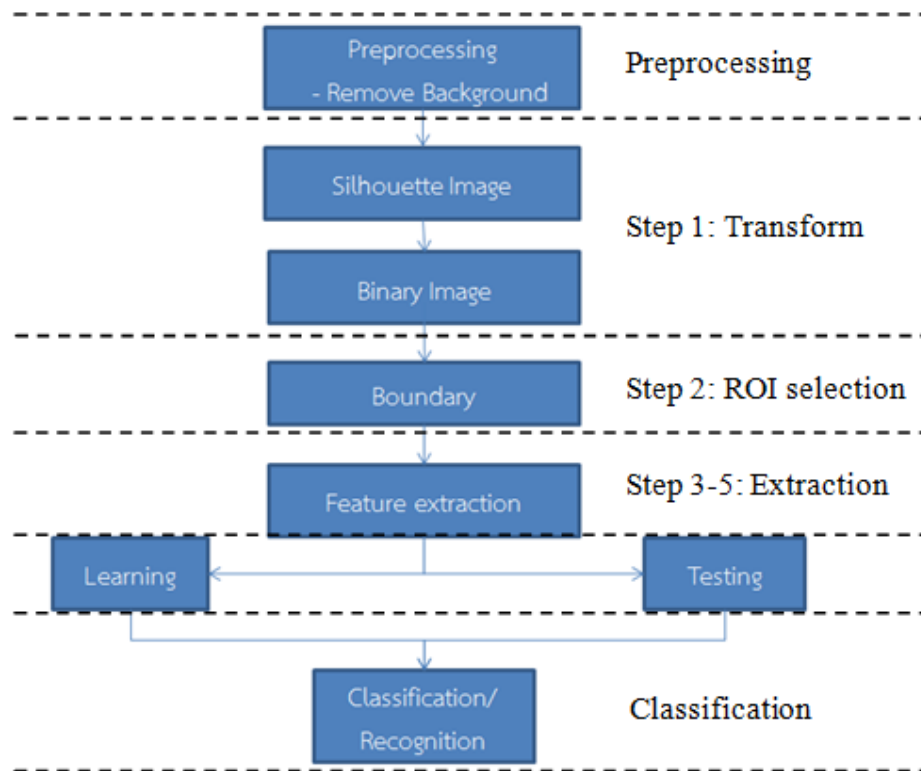
Figure 3.1 General concept of an algorithm for warship classification

3.4 Transition Scaling and Rotation Feature Extraction

Our method starts with extracting the superstructure of an image by transforming the image to a binary image and calculating the different of tangents along the boundary of the binary image. To fix the Region-of-Interest (ROI) and avoid noise, the ratio and PAA method give average angles to DTW and k-NN by working with different of tangents data for classification, as detailed below.

Step 1: Transform image to binary image. In the binary image, "0" represents black or the object area and "1" represents white or the background area.

Step 2: ROI is used to find the boundary by contour tracing [49]. The goal of contour tracing is to find an external contour at a given pixel, named S. At this pixel, we first identify S as the start point. Contour tracing will find the next contour point next to S by tracing the outline in a counterclockwise direction. The next point is T. We then continue to execute tracing to find the next contour point from T until both of the following two conditions hold: (i) the tracing outputs S again, and (ii) the next contour point of S is T again. The output of this contour tracing technique is a set of boundary coordinates of the input image. Reference [50] obtains geometric shape information and edge points of objects. We followed the procedures outlined by [49] and [50] to outline the outer boundary of images.
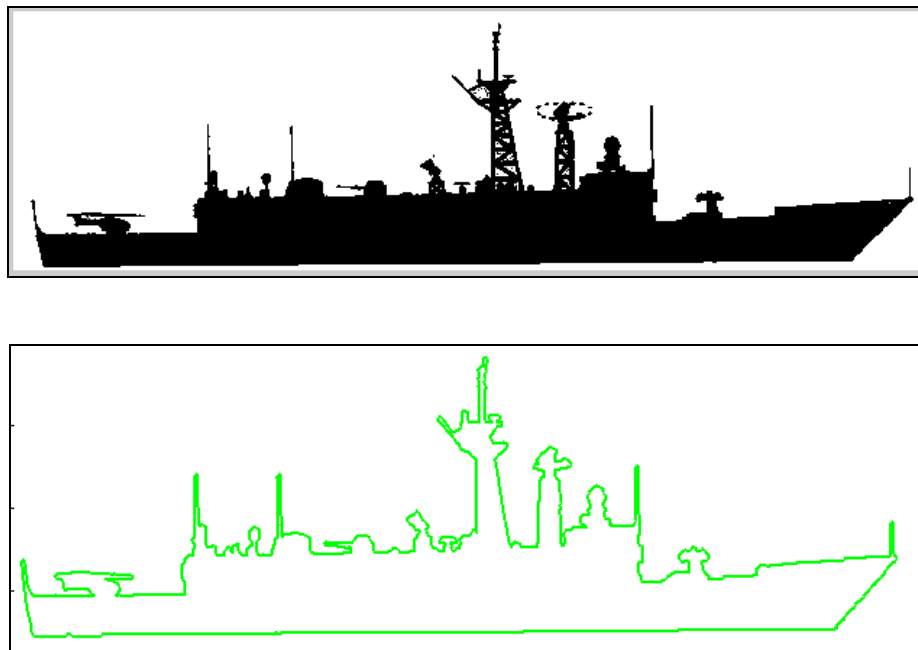
Figure 3.2 Ship silhouette (top) and its boundary (bottom)

- ***Transition and Scaling***

Step 3: The outer boundary of the binary image as shown in Figure 3.2 is created from the contour tracing algorithm outlined in Step 2 in eight-connected binary images. This function returns a Q-by-2 matrix, where Q is the number of boundary pixels for the region.
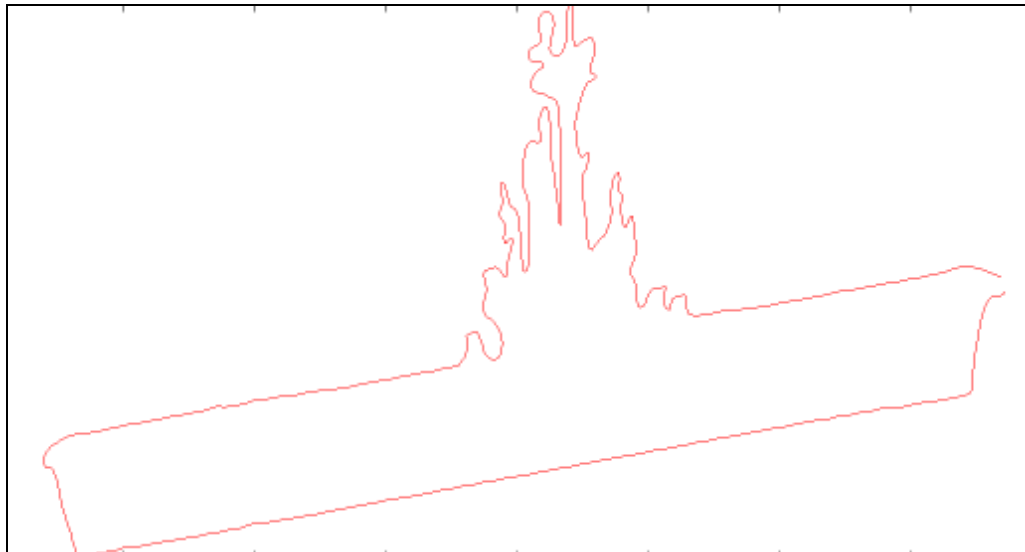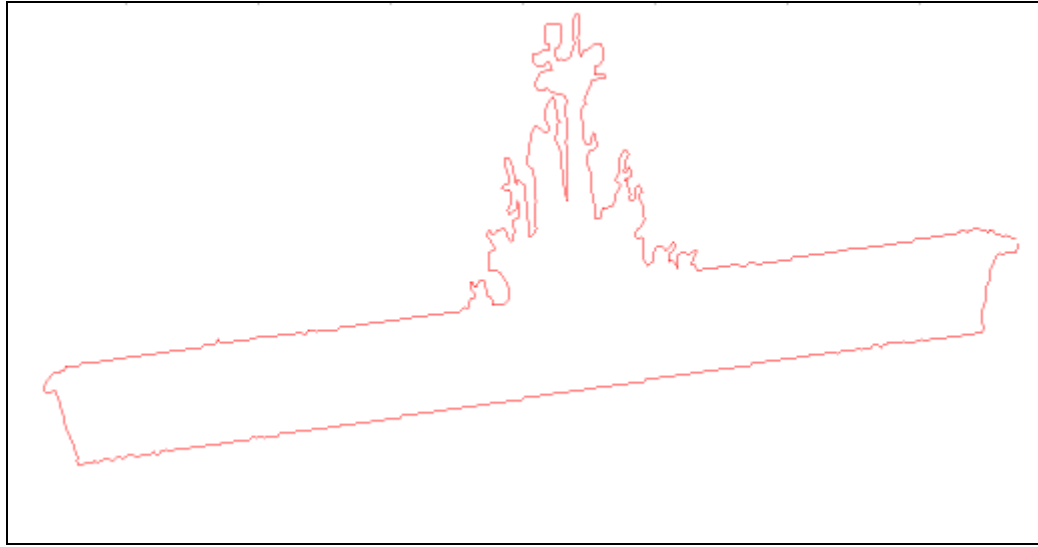
Figure 3.3 Convolution, reducing the noise from original (top) and

smoothing the boundary with convolution (bottom)

.

The matrix holds the row and column co-ordinates of the boundary pixels.
The co-ordinates of pixels of outer boundary are:

$$Q = (X_1, Y_1), (X_2, Y_2), \ldots (X_n, Y_n) \tag{13}$$

In addition, this step, we used 1 x 5 windows size convolution technique [35, 46] to smooth the boundary from the noise in situation of rotation, since next step, tangent angle is sensitive to noise. Figure 3.3 shows that smoothing the boundary can reduce the noise.

Instead of using co-ordinate, we use tangent angle as shape representation and description. We applied the algorithm used in [51] and [52] by calculating the tangent in degree of angle. With this algorithm, the translation position of an image with the same feature can be extracted. The tangent angle is invariant with change of scale. By calculating the tangent in degrees, we can fix the tangents of π/2 and 3π/2 that are not defined in radians. The tangent between two co-ordinates is:

$$T_n = (Y_{n+1} - Y_n) / (X_{n+1} - X_n) \tag{14}$$

$$T = (T_1, T_2, T_3 .....T_n) \tag{15}$$

"*T*" is the set of tangents between two co-ordinate points along the boundary.
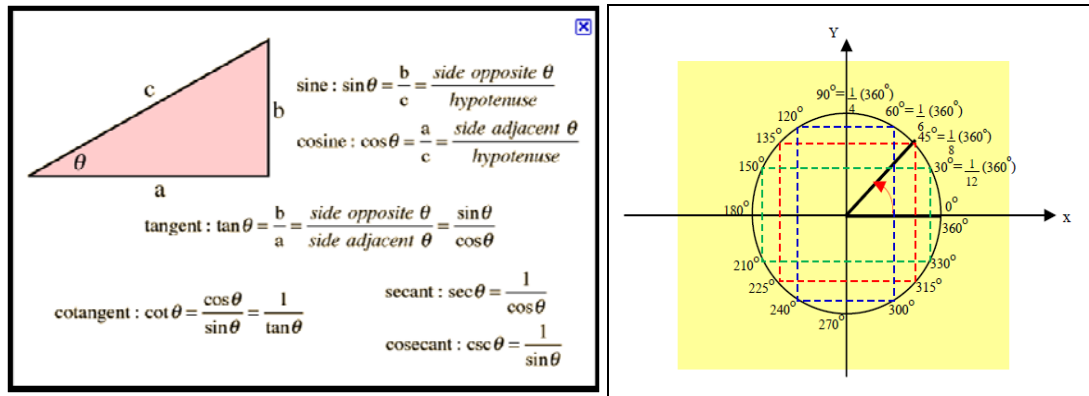
Figure 3.4 Tangent degree calculated

- ***Rotation***

Step 4: To work with rotation, we calculate the set of different of tangents and use this to define the description as equation:

$$DT_n \ = (\ T_{n+1}, \ - \ T_n) \tag{16}$$

$$DTS \ = (DT_1, \ DT_2, \ DT_3 \ ..... DT_n) \tag{17}$$

DT is the different of tangents in each tangent point and *DTS* is a set of *DT*.

Step 5: We apply PAA to reduce the data dimensions to speed up the distance function, as shown in Figure 3.5 The formula for average of angle of tangent in length "n" is shown below:

$$D_{avg} = ((DT_1 + DT_2 + DT_3 + ... + DT_n) \ /n) \tag{18}$$

$$D_{paa} \ = (D_{avg1}, \ D_{avg2}, \ D_{avg3} \ ,..... \ , \ D_{avgn}) \tag{19}$$

D_{avg} is the average of tangent of length "*n*" and D_{paa} is the set of D_{avg} that we extracted from the ship silhouette. We use D_{paa} as data for distance function (DTW) classified by k-NN as outlined in the following section.
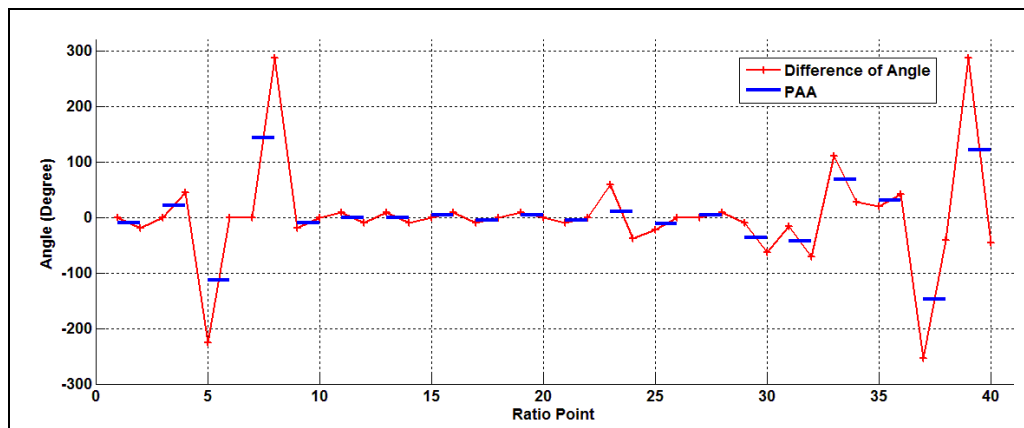
Figure 3.5 Different of Tangent and its PAA

3.5 Similar Measurement and Classification

Since we have a set of averages of different of tangent angle (DOT) that is invariant for translation, scaling, and rotation, we can now measure the similarities between a known ship and a ship with an unknown class. Using of DTW for the distance measurement results in an order similar to that of k-NN for classification of the unknown ship.

In this step, due to the drawback of k-NN, the training process on all data set that would be slow. On the future work, we plan to use two levels of classification for reduction of training data set, process as shown in Figure 3.6. First classifier would be using the circularity, if accepted; the next classifier would be classified.
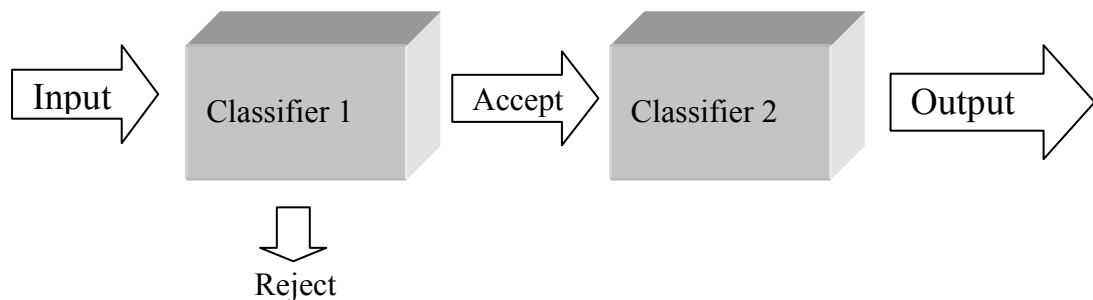
Figure 3.6 Two levels of classification

3.6 Basic Concept

Figure 3.7 shows that the data from the tangent angle function of three geometric images had a different of tangent angles because of translation, rotation, and scaling of images (a, b, and c). A plot of the tangent angles that shown in (d). The output data obtained were using DOT as shown in (e), where the results are similar.

With general concept as brief, we have applied to the experimental: Classification and Cross-validation.

(a) Original   (b) Rotation   (c) Scaling
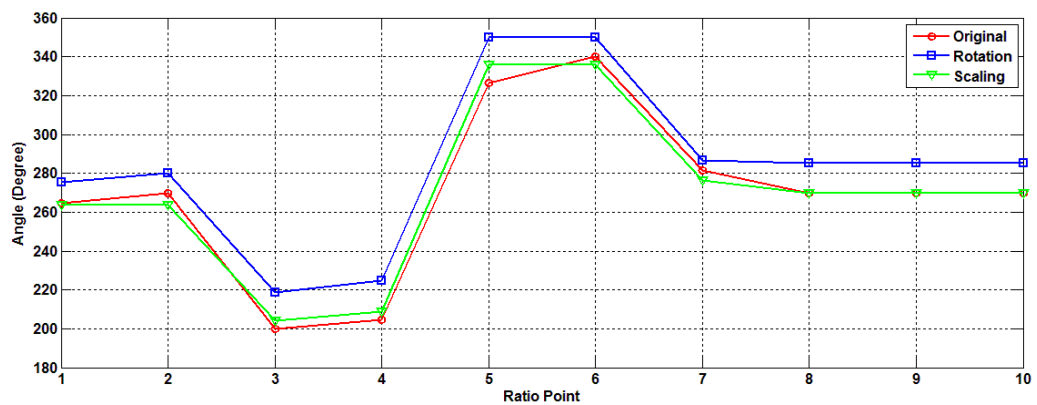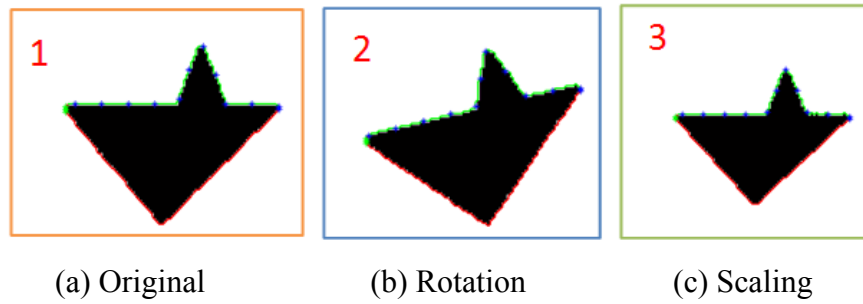
(d) Tangent angle with PAA
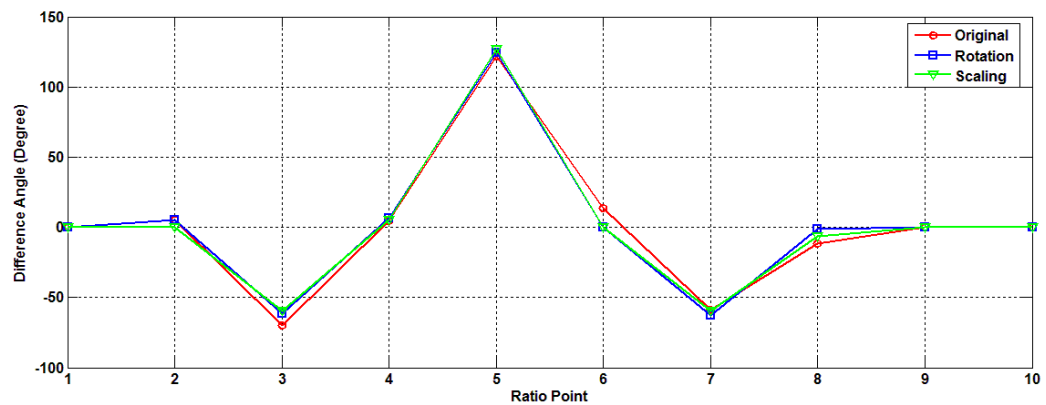
(e) Different of tangent angle with PAA

Figure 3.7 Different of tangent angle with PAA is invariant for translation, rotation and scaling

3.7 Classification and Cross-validation

3.7.1 Dataset

We tested our method with original images of 8 types and 70 Classes of warships and generated new images by translation (shift to 10 position for each), reduced in size from original (resize to: 0.7, 0.8, 0.9, 1, 1.2, 1.3, 1.4, 1.5, 1.6, 1.7 times) and rotated (turn angle to: 2, 4, 6, 8, 10, -2, -4, -6, -8, -10 degree), the total is 30 images for each class, the detail shown in Table 3.1. A total of images are 2,100 images comprised the dataset. Figure 3.9 shows examples of warship images used.

3.7.2 Method

The experiment used 2,100 images and used stratified 10-fold cross-validation (CV) [53] that divided all data into 10 equal parts. Each part in turn is used as a test set and the other 9 parts are used as a training set. Every part would turn to test set; the total of test process would be 10 times. The total number of instances correctly classified is divided by the total number of all instances to give an overall level of predictive accuracy. The procedure of stratification is to ensure that the random sampling is done in such a way as to guarantee that each class (of warship) is properly represented in both training and test sets [53, 55].

Table 3.1 Generated of warship images

Ship Type	No. of Class	Generate (images)			Total of images
		Translation	Scaling	Rotation	
Aircraft Carriers	9	90	90	90	270
Amphibious	5	50	50	50	150
Corvettes	12	120	120	120	360
Cruisers	10	100	100	100	300
Destroyers	12	120	120	120	360
Frigates	10	100	100	100	300
Mine Warfare	6	60	60	60	180
Patrol Forces	6	60	60	60	180
Total	70	700	700	700	2,100

Figure 3.8 shows the example of stratified 5-fold cross-validation (Figure 3.8 (a)) and stratified 4-fold cross-validation (Figure 3.8 (b)).
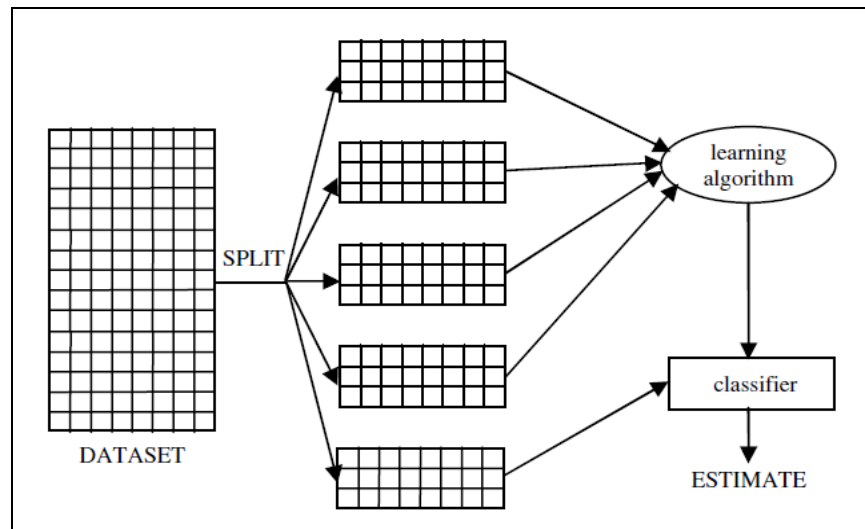
(a) Stratified 5-fold cross-validation
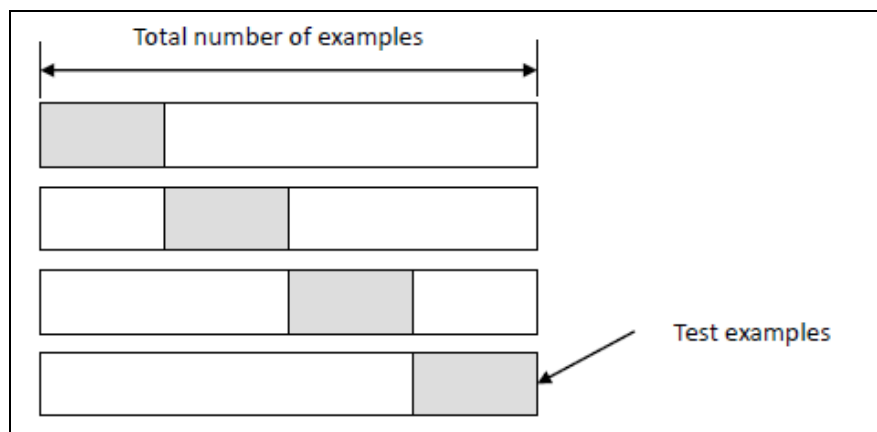
(b) Stratified 4-fold cross-validation

Figure 3.8 Stratified Cross-validation

With our method, the experiment is performed and the result and analysis will be discussed in Chapter VI.

Aircraft Carriers

Cruisers

Destroyers

Frigates

Figure 3.9 Examples of warship images

Corvettes

Patrol Forces

Mine Warfare Forces

Amphibious
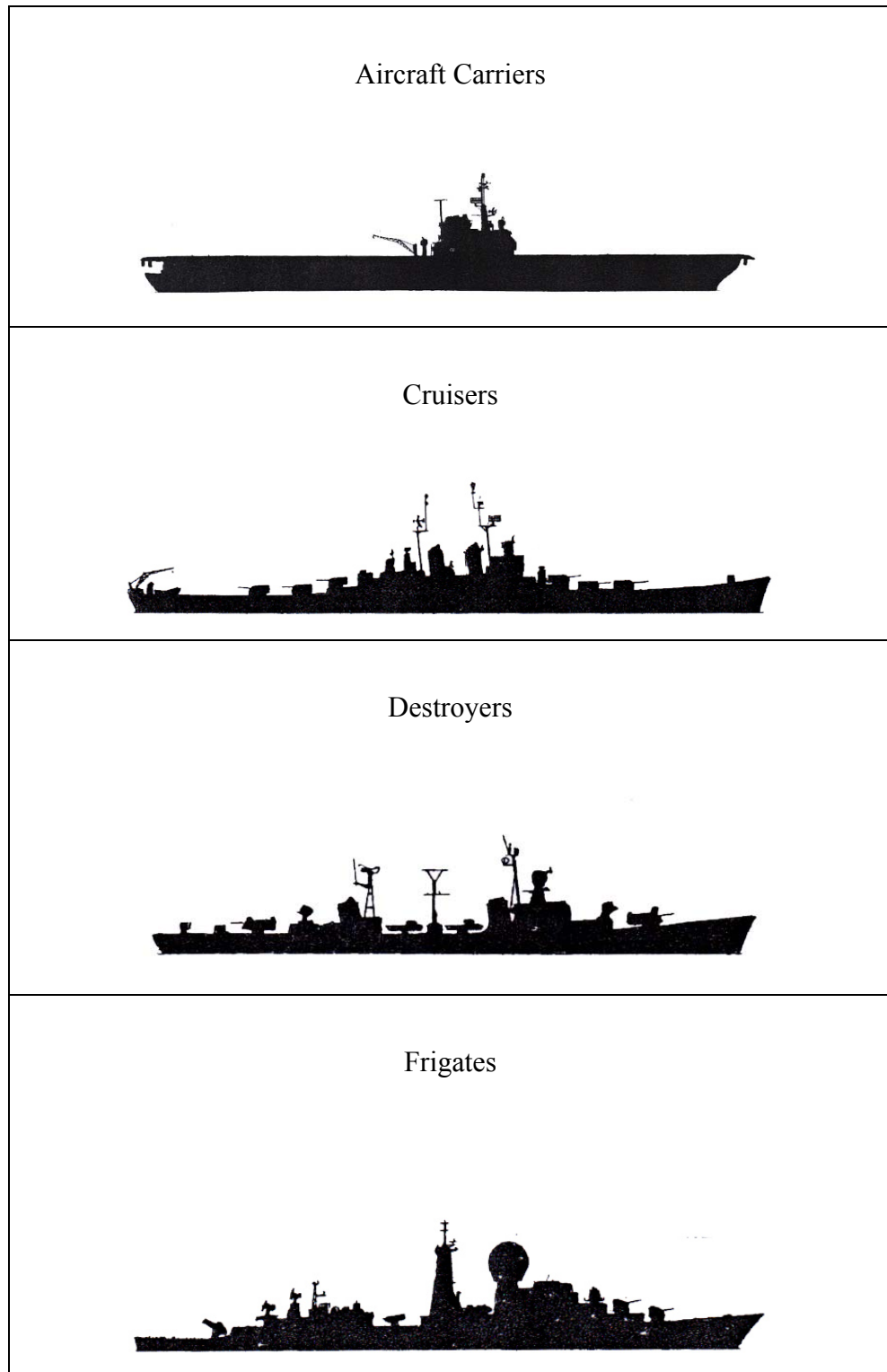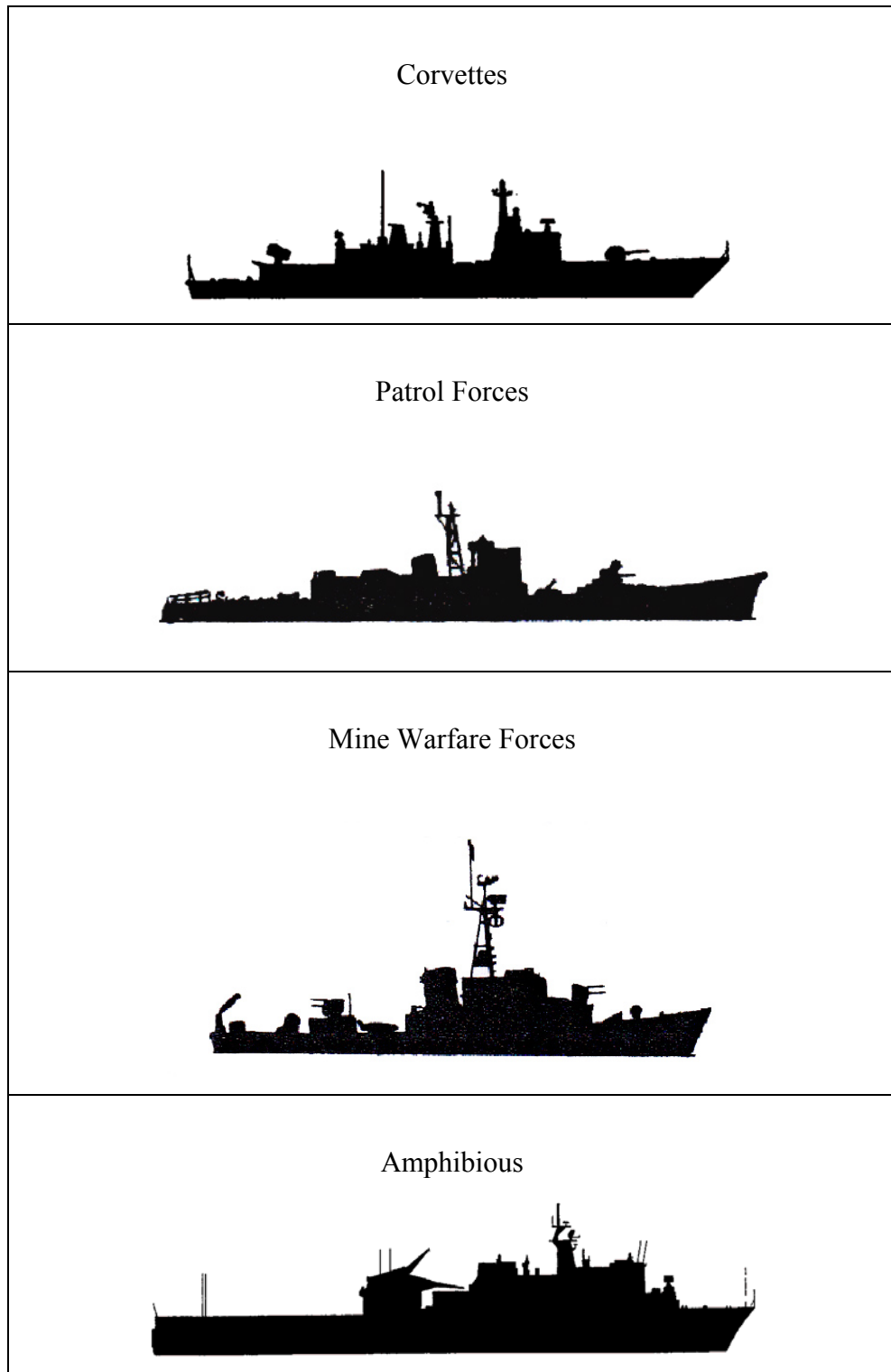
Figure 3.9 Examples of warship images (cont.)

CHAPTER IV
RESULTS AND DISCUSSION

A classification of warship from distant view was studied. This chapter discussed result of our experiment, the Classification and cross-validation, t-test samples, confusion matrix and Receiver Operating Characteristics (ROC).

4.1 Classification and cross-validation (CV)

We tested our method with original images of eight types and 70 Classes of warships, reduced in size and rotated. A total of 2,100 images comprised in the dataset.

The results of the experiment prove that our method provide high accuracy in classification under translation, scaling, and rotation, in each class of ships. The average of accuracy of DTW and ED with stratified 10-fold CV and 1-NN are shown in Table 4.1 and Table 4.2.

Table 4.1 Average of accuracy of DTW and 1-NN with stratified 10-fold CV

Ship Type	No. of classes	No. of images	TRUE	FALSE	Accuracy (%)
Aircraft Carriers	9	270	259	11	95.93
Amphibious	5	150	144	6	96.00
Corvettes	12	360	344	16	95.56
Cruisers	10	300	285	15	95.00
Destroyers	12	360	345	15	95.83
Frigates	10	300	288	12	96.00
Mine Warfare	6	180	174	6	96.67
Patrol Forces	6	180	175	5	97.22
Total	70	2,100	2014	86	

Table 4.2 Average of accuracy of ED and 1-NN with stratified 10-fold CV

Ship Type	No. of classes	No. of images	TRUE	FALSE	Accuracy (%)
Aircraft Carriers	9	270	253	17	93.70
Amphibious	5	150	137	13	91.33
Corvettes	12	360	330	30	91.67
Cruisers	10	300	258	42	86.00
Destroyers	12	360	348	12	96.67
Frigates	10	300	286	14	95.33
Mine Warfare	6	180	172	8	95.56
Patrol Forces	6	180	165	15	91.67
Total	70	2100	1949	151	

Figure 4.1Accuracy of ED and DTW

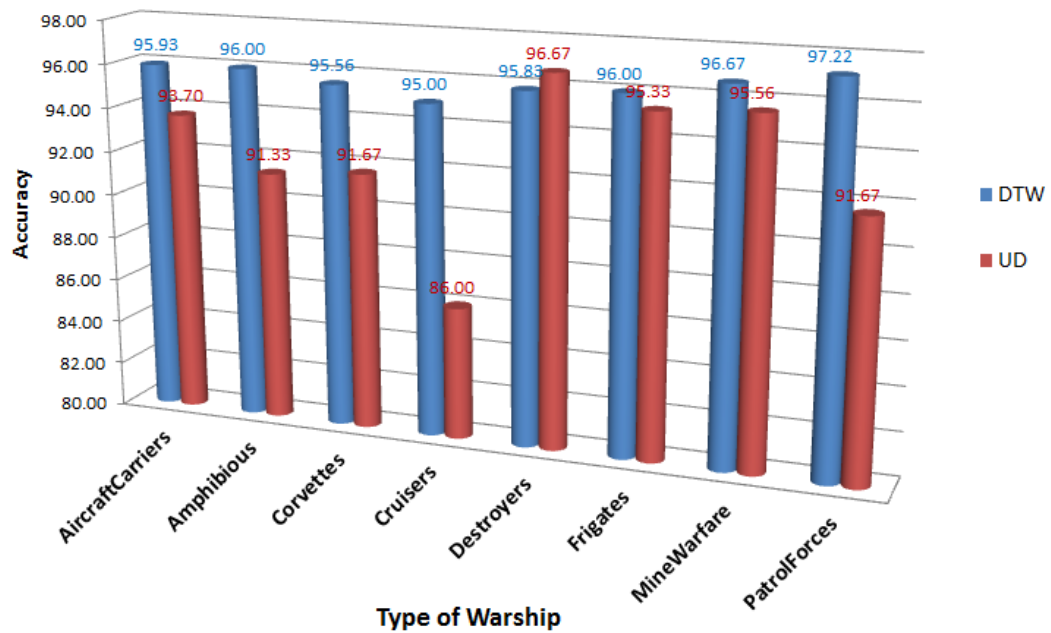In figure 4.1, the average of accuracy in Table 4.1 and 4.2 are compared. The comparison of classification rate results between ED and DTW with 1-NN shown in Figure 4.1. The average of DTW accuracy is 96.03 % that greater than the average

of ED accuracy at 92.74 %. But Destroyers type, the ED accuracy is better than DTW accuracy. We found that some types, DTW and ED gave similar classification rates.

However, to compare the accuracy of DTW and ED, the hypothesis testing calculated with SPSS by using a paired t-test for dependent samples because we compared DTW and ED with the same group of data.

The null H_o is the average of the DTW's accuracy (μ_1) and ED's accuracy (μ_2) are equal (H_o: $\mu_1 = \mu_2$), and the research H_1 is that DTW's accuracy had greater than ED's accuracy (H_1: $\mu_1 > \mu_2$).

Table 4.3 Paired t test Samples Statistics of Accuracy of ED and DTW

Group	Mean	SD	Paired Samples Correlations				
			Mean	SD	t	df	Sig.(2-tailed)
ED	92.80	2.93	3.09	2.99	3.27	9	0.01
DTW	95.90	2.85					

Table 4.3 shows that the accuracy's mean of the DTW equals to 95.90, with Standard Deviation of 2.85 while the accuracy's mean of ED is equal to 92.80 with Standard Deviation of 2.93. The calculated t is equal to 3.27 that greater than 1-tailed t-test ($t_{(0.01,9)}$) that equal to 2.82. We found that the accuracy's mean of the DTW is significantly greater than the accuracy's mean of ED. Therefore we would reject the null hypothesis (H_o) and would, therefore, accept the alternative hypothesis (H_1). That means DTW's accuracy is greater than ED's accuracy at significant (2-tailed) which is equals to 0.01.

In confusion matrix, the performance of classification success is based on four numbers obtained from applying the classifier to the test set. These numbers are called true positives *TP*, false positive *FP*, true negatives *TN*, and false negatives *FN* [55]. The results are counted and entered in a 2 x 2 table. However, in our case, we test experiment with 70 classes of warship, the table is 70 x 70 which is called the confusion matrix of multi classes or several classes. The confusion matrix of 70 classes is shown as follows:

Two-Class Problem

		Prediction		
		c^+	c^-	Total
Actual	c^+	TP	FP	N^+
	c^-	FN	TN	N^-
	Total	$\hat{N}^+$	$\hat{N}^-$	N

(a)

Several-Class Problem

		Prediction					
		c_1	c_2	c_3	$\ldots$	c_n	Total
Actual	c_1	TP_1	FN_{12}	FN_{13}	$\ldots$	FN_{1n}	N_1
	c_2	FN_{21}	TP_2	FN_{23}	$\ldots$	FN_{2n}	N_2
	c_3	FN_{31}	FN_{32}	TP_3	$\ldots$	FN_{3n}	N_3
	$\ldots$	$\ldots$	$\ldots$	$\ldots$	$\ldots$	$\ldots$	$\ldots$
	c_n	FN_{n1}	FN_{n2}	FN_{n3}	$\ldots$	TP_n	N_n
	Total	$\hat{N}_1$	$\hat{N}_2$	$\hat{N}_3$	$\ldots$	$\hat{N}_n$	N

(b)

Figure 4.2 Confusion matrix of two classes (a) and multi classes (b) problem

Figure 4.3 Confusion matrix score for multi classes problem

Table 4.4 Confusion matrix of DTW

Actual class	Predicted class								
	AircraftCarriers	Amphibious	Corvettes	Cruisers	Destroyers	Frigates	MineWarfare	PatrolForces	Total
AircraftCarriers	265	5	0	0	0	0	0	0	270
Amphibious	4	144	0	0	0	2	0	0	150
Corvettes	0	2	351	0	3	2	0	2	360
Cruisers	0	0	0	290	5	5	0	0	300
Destroyers	0	1	0	4	351	4	0	0	360
Frigates	2	0	1	1	6	290	0	0	300
MineWarfare	0	1	1	0	2	1	175	0	180
PatrolForces	0	0	1	0	1	1	1	176	180
Total	271	153	354	295	368	305	176	178	

In our experiment 70 x 70 confusion matrix was created. However, to display in the thesis we formed new confusion matrix by the type of warship; 8 x 8 as Table 4.4 (DTW) and Table 4.5 (ED).

Table 4.5 Confusion matrix of ED

Actual class	Predicted class								
	AircraftCarriers	Amphibious	Corvettes	Cruisers	Destroyers	Frigates	MineWarfare	PatrolForces	Total
AircraftCarriers	260	5	3	1	0	1	0	0	270
Amphibious	12	137	0	0	0	0	0	1	150
Corvettes	11	7	338	0	1	3	0	0	360
Cruisers	15	13	5	259	1	2	1	4	300
Destroyers	6	2	1	0	348	2	0	1	360
Frigates	9	5	0	0	0	286	0	0	300
MineWarfare	5	0	2	0	0	1	172	0	180
PatrolForces	6	5	3	0	1	0	0	165	180
Total	324	174	352	260	351	295	173	171	

Table 4.4 and 4.5 shown the confusion matrix of DTW and ED, we found that even every type has a high correct classified. However, some type of warship was classified to other types. The Receiver Operating Characteristics (ROC) used to measure the false classified in next analysis.

4.2 ROC (Receiver Operating Characteristics)

Accuracy of the method has shown in Table 4.4 and 4.5 with good classification rate. However, the performance of classification using only the accuracy is not enough [54, 55]. The ROC is also another one of good performance measurement. Table 4.6 shows the comparison of the value of TP rate and FP rate between ED and DTW and ROC graphs were plotted as shown in Figure 4.4.

Table 4.6 TP, TN, FP and FN of DTW and ED

Ship Type	DTW				ED			
	TP	TN	FN	FP	TP	TN	FN	FP
Aircraft Carriers	265	1824	5	6	260	1766	10	64
Amphibious	144	1941	6	9	137	1913	13	37
Corvettes	351	1739	7	3	338	1726	22	14
Cruisers	290	1795	10	5	259	1799	41	1
Destroyers	351	1723	9	17	348	1737	12	3
Frigates	290	1785	10	15	286	1791	14	9
Mine Warfare	175	1919	5	1	172	1919	8	1
Patrol Forces	176	1918	4	2	165	1914	15	6

False positives (also known as *Type 1 Errors*) occur when instances that should be classified as negative, but are classified as positive.

False negatives (also known as *Type 2 Errors*) occur when instances that should be classified as positive, but are classified as negative.

Depending on the application, errors of these two types are more or less important. Here we may be willing to accept a high proportion of false negatives, but probably do not want too many false positives [54].

Table 4.6 shows two errors of our results in each type of warship. DTW has all of FN and some FP smaller than ED, but some of FP is greater.

From Table 4.6, the accuracy, precision and recall are calculated:

ALL = TP + TN + FN + FP

Accuracy = TP + TN / ALL

Precision = TP / TP + FP

Recall = TP / TP + FN

The result as follow:

- DTW

      - Accuracy = 0.993

      - Precision = 0.972

      - Recall = 0.973

- ED

    - Accuracy = 0.983

    - Precision = 0.935

    - Recall = 0.935

For plotting the ROC, the TP rate and FP rate are calculated from Table 4.6 as shown in Table 4.7.

Table 4.7 TP rate and FP rate of DTW and ED in each type

Ship Type	DTW Rate		ED Rate	
	TP	FP	TP	FP
AircraftCarriers	0.981	0.003	0.963	0.035
Amphibious	0.960	0.005	0.913	0.019
Corvettes	0.980	0.002	0.939	0.008
Cruisers	0.967	0.003	0.863	0.001
Destroyers	0.975	0.010	0.967	0.002
Frigates	0.967	0.008	0.953	0.005
MineWarfare	0.972	0.001	0.956	0.001
PatrolForces	0.978	0.001	0.917	0.003
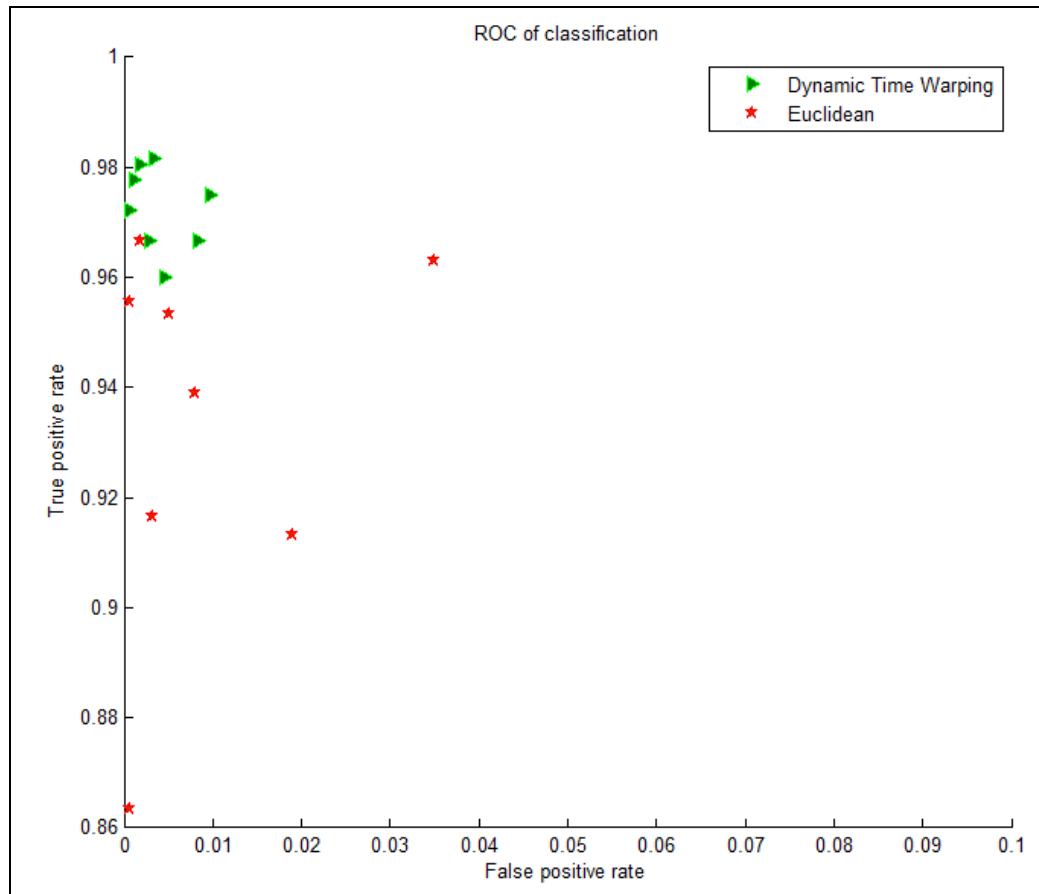
Figure 4.4 ROC of ED and DTW

Measuring the performance of two classifier or method in multiclass problem, via predictive accuracy on its own is not a reliable indicator of a classifier's effectiveness [54].   The ROC in Figure 4.4 is discrete and hard to measure the performance. However, AUC (Area Under a ROC Curve) is useful for this.

In Figure 4.5 and 4.6, the ROC graph and AUC are generated by online application (http://www.vassarstats.net/roc1.html) by Department of Radiology, Kurt Rossmann Laboratories, University of Chicago [56]. The AUC computed using algorithm [57].
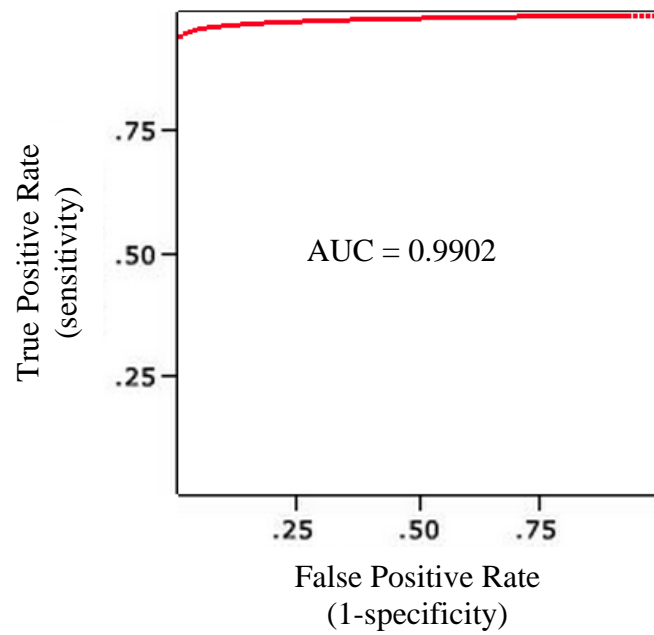
(a) ROC of DTW, AUC = 0.9902
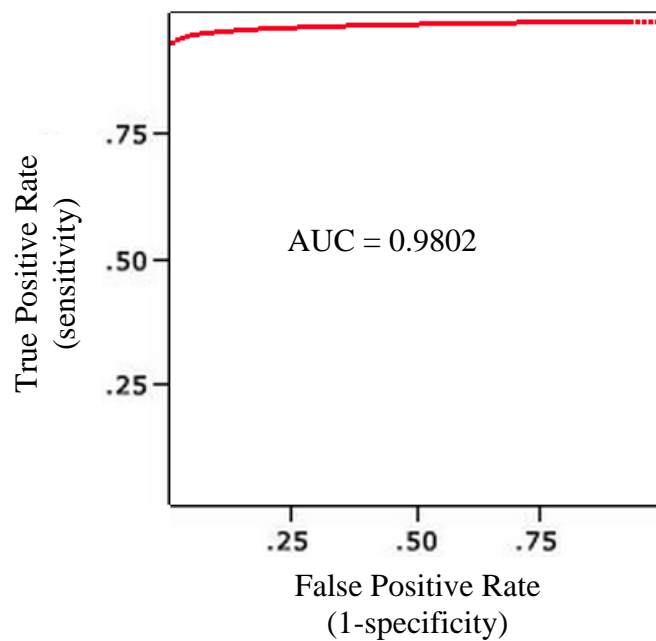
(b) ROC of ED, AUC = 0.9802

Figure 4.5 AUC of DTW (a) and ED (b) by ROC curve analysis software [56]

	DTW	ED
number of actually negative cases	14702	14700
number of actually positive cases	2098	2100
area under curve	.9902	.9802
standard error	0.0015	0.0021
difference: $area_A - area_B$	0.01	
standard error of the difference	0.0026	
z	3.8046	
P: non-directional (two-tailed)	0.000142	
P: directional (one-tailed)	0.000071	

Figure 4.6 Significance of the difference AUC

Significance of the difference between the areas that lie under the curves in Figure 4.5 (a) and (b) used to measure the performance of classifier and show that the areas under ROC curves of DTW (Figure 4.5 (a)) is with a greater area and therefore better average performance than ED (Figure 4.5 (b)).

This chapter describes the result of our experiment; we found that the experiment has given good result. The performance of classification by using DTW to measure the similarity gives high accuracy. The limitation is a small number of images that were used in the experiment as samples. The 2 level of classifier may give fast in training process that can apply to the real world application. However, this issue could be solved through future work.

CHAPTER V
CONCLUSION

Classification of an object as a warship from a distant view is one of the important information. Our studies classify warship images which is invariant under translation, scaling, and rotation.

5.1 Conclusion

Based on distant view image, we present the Difference of Tangent (DOT) angle. We proved that the DOT is invariant under translation, scaling, and rotation. And by using DTW and 1-NN, the method provided good classification rate.

We also found that good feature extraction technique could give good data that simple to similarity measurement and classification. As we could see in Destroyers type, the ED's accuracy was better than DTW's accuracy. We found that some types, DTW and ED gave similar classification rates that mean when we have good feature extraction, we could use the ease similarity measure method such the ED that has advantage in cost computation.

The computation can be reduced by using two levels of classification that we will give to the future work. However, in real images, the dynamic background of images needs more study.

5.2 Future work

5.2.1 To apply this method with large number of real images.

5.2.2 To study base on dynamic change of background images.

5.2.3 To study on two levels of classification.

REFERENCES

1   Renner S. Building Information Systems for Network-Centric Warfare. The MITRE Corporation; MA; 2003.

2   Gouaillier V., Gagnon L. Ship Silhouette Recognition Using Principal Components Analysis. SPIE Proc. #3164; CA; 1997.

3   Pastina D. C. Multi-feature based automatic recognition of ship targets in ISAR images. IEEE; University of Rome; 2008.

4   Rice F., Cooke T., Gibbins D. Model based ISAR ship classification. Digital Signal Processing 16; 2006. p. 628-637.

5   Knapskog A. O. Classification of Ships in TerraSAR-X Images Based on 3D Models and Silhouette Matching. EUSAR. Norway; 2010.

6   Zhongliang Q., Wenjon W. Automatic Ship Classification by Superstructure Moment Invariants and Two-stage Classifier. ICCS/ISITA. Singapore; 1992. p. 544-547.

7   Alves J., Herman J., Rowe N. C., "Robust Recognition of Ship Types from an Infrared Silhouette", Naval Postgraduate School, CA, 2004.

8   Araghi L. F., Kholooade H., Arvan M. R. Ship Identification Using Probabilistic Neural Network (PNN). IMECS; 2009, p.326-329.

9   Lobo V. J., Bandeira N., Moura-Pires F. Ship recognition using Distributed Self Organizing Maps. EANN 98. PORTUGAL; 1998.

10 Arantes A. et al. Ship's Classification by its Magnetic Signature. IEE International; 1998.

11 Talbot-Booth, David G. Warship Identification. United States Naval Institute, Maryland: Annapolis; 1971.

12 Bizer M. J. A Picture-descriptor Extraction Program Using Ship Silhouettes, DTIC. Monterey, CA; 1989.

13 Inggs M. R., Robinson A. R. Neural Approaches to Ship Target Recognition. IEEE International Radar Conference; 1995. p.386-391.

14 Selvi M. U., Kumar S. S. A Novel Approach for Ship Recognition using Shape and Texture. IJAIT Vol.1 No.5; 2011. p.23-28.

15 Feineigle P. A., Morris D. D., Snyder F. D. Ship Recognition Using Optical Imagery for Harbor Surveillance. AUVSI. Washington DC; 2007.

16 Luna A. E., et al. A decision support system for ship identification based on the curvature scale space representation. Madrid, Spain; 2005.

17 Nor S. B. S Vessels Classification. University Technology Malaysia; 2006.

18 Ronald P., Mannes P. Comparison of Silhouette Shape Descriptors for Example-based Human Pose Recovery. University of Twente, Netherlands; 2005.

19 Javier C., Josep A., Fernando D. T. Robust Normalization of Silhouettes for Recognition Applications. Ramon Liull University; 2003.

20 Wael A., Christopher S. Hidden Markov Models for Silhouette Classification. University of New Mexico; 2001.

21 Josef B. A Systematic Introduction to Image Processing and Computer Vision. Springer-Verlag. Berlin Heidelberg; 2006.

22 Irene R. K. Shape and Context. Tuwien; 2009.

23 Sven L. A Survey of Shape Analysis Techniques. Pattern Recognition; 1996.

24 Dengsheng Z., Guojun L. Review of shape representation and description techniques. Pattern Recognition. 37; 2004. p.1-19.

25 ANM E. H. Shape Analysis and Measurement for the HeLa cell classification of cultured cells in high throughput screening. University of Skövde, Sweden;, 2006.

26 Yang M., Kpalma K., Rosin J. A Survey of Shape Feature Extraction Techniques. Pattern Recognition Techniques. I-Tech, Austria; 2008.   p.43-89.

27 Aaron S. K. et al. Characterizing Structure Through Shape Matching and Applications to Self Assembly. University of Michigan; 2010. p.1-19.

28 Achard, C., Devars, J., Lacassagne, L. Object Image Retrieval with Image Compactness Vectors. Proceedings of the International Conference on Pattern Recognition (ICPR'00) 1051-4651/00; 2000.

29 Tak-chung F. A Review on Time series Data mining. Engineering application of artificial intelligence 24; 2011. p.164-181.

30 Hui D. et al. Querying and Mining of Time Series Data: Experimental Comparison of Representations and Distance Measures. PVLDB'08. New Zealand; 2008. p.1542-1552.

31 Hailin L., Chonghui G., Wangren Q. Similarity measure based on piecewise linear approximation and derivative dynamic time warping for time series mining. Expert system with applications; 2011. P.14732-43.

32 Aparna R., Bincy G., Mathu T. Survey on Common Data Mining Classification Techniques. International Journal of Wisdom Based Computing, Vol.2(1). India; 2012. p.12-15.

33 Kotsiantis S. B. Supervised Machine Learning : A Review of Classification Techniques. University of Peloponnese, Greece; 2007. p.249-268.

34 Thair N. P. Survey of Classification Techniques in Data Mining. IMECS 2009. Hong Kong; 2009.

35 Ratika P., Shikhar K., Ruchika A., Mohan P., Ghose M. K. Contour Line Tracing Algorithm for Digital Topographic Maps. International Journal of Image Processing (IJIP), Volume (4). Issue (2). p. 156-163.

36 Keogh E. J., Pazzani M. J. Scaling up Dynamic Time Warping for Data mining Applications. Irvine, University of California; 2000.

37 Ratanamahatana A. C. et al. Mining Time series Data. Riverside, California.

38 Zhang Y., Glass J. A piecewise Aggregate Approximation Lower-Bound Estimate for Posteriorgram-based Dynamic Time Warping. ISCA. Florence, Italy; 2011. p.1909-1912.

39 Senin P. Dynamic Time Warping Algorithm Review. Honolulu. University of Hawaii at Manoa; 2008.

40 Keogh X. Xi, E., Shelton C., Wei L. Fast Time Series Classification Using Numerosity Reduction. International Conference of Machine Learning. Pittsburgh, PA; 2006.

41 Islam K. T. et al. Enhanced 1-NN Time Series Classification Using Badness of Records. in Proc. ICUIMC, Suwon, South Korea; 2008.

42 Vit N., Ratanamahatana A. C. Learning DTW Global Constraint for Time Series Classification.

43 Elkan C. Nearest Neighbor Classification. UCSD; 2011.

44 Weis M., Rumpf T., Gerhards R., Plumer L. Comparison of different classification algorithms for weed detection form images based on shape parameters. University of Hohenheim, Germany; 2009.

45 Hsu H., Yang A. C., Lu M. KNN-DTW based Missing Value Imputation for Microarray Time Series Data. Journal of Computers, Vol.6 No.3; 2011. p. 418-425.

46 Mark S. Nixon, Alberto S. A. Feature Extraction and Image Processing. 2002

47 Saunders S. Jane's Fighting Ships 2010-2011; 2011.

48 Anthony J. Watts. Jane's Warship Recognition Guide. New York, NY: Collins, 2006.

49 Chang F., Chen C. A Component-Labeling Algorithm Using Contour Tracing Technique", IEEE Transactions on Document Analysis and Recognition, 2003.

50 Talu M. F., Turkoglu I. A Novel Object Recognition Method Based on Improved Edge Tracing for Binary Images. IEEE; 2009.

51 Feschet F., Tougne L. Optimal Time Computation of the Tangent of a Discrete Curve: Application to the Curvature. DGCILNCS 1568. Bron, France; 1999. p. 31-40.

52 Matas J., Shao Z., Kittler J. Estimation of Curvature and Tangent Direction by Median Filtered Differencing. In Conf. on Image Analysis and Processing, San Remo; 1995. p.13-15.

53 Ian H. W., Eibe F. Data Mining Practical Machine Learning Tool and Techniques; 2005

54 Max B. Principles of Data Mining, Springer, 2007.

55 Charles E. , "Evaluating Classifiers", UCSD, 2012

56 Kurt Rossmann. ROC application. Department of Radiology, Laboratories, University of Chicago [Online]. Available from: http://www.vassarstats.net/roc1.html [Accessed 2013 Mar 25].

57 Tom Fawcett, "ROC Graphs: Notes and Practical Considerations for Researchers", Kluwer Academic Publishers, 2004, pp. 1-37

BIOGRAPHY

NAME	Sub.Lt. Buncha Chuaysi
DATE OF BIRTH	15 January 1973
PLACE OF BIRTH	Sa Kaeo, Thailand
INSTITUTIONS ATTENDED	Ramkhamhaeng University, 1993-2001

Bachelor of Art (Political Science)

Nakhon Pathom Rajabhat University,

2009-2010

Bachelor of Science (Information

and Communication Technology)

Mahidol University, 2011-2013

Master of Science (Technology

Information System Management)

RESEARCH GRANTS The 60th Year Supreme Reign of His

Majesty King Bhumibol Adulyadej

Scholarship

HOME ADDRESS 67/145 Phuttamonthon 3 Rd, Sala

Thammasop, Thawi Watthana,

Bangkok 10170

Tel. 08-7075-6454

E-mail:buncha.c@navy.mi.th

PUBLICATION / PRESENTATION Warship Classification from Distant View

Using Dynamic Time Warping and k-NN,

2012 International Workshop on Smart

Info-Media System in Asia (SISA 2012),

Bangkok, Thailand